AD-A171 635 ELECTRON MICROSCOPY OF INTRACELLULAR PROTOZOA(U) CASE WESTERN RESERVE UNIV CLEVELAND OHIO INST OF PATHOLOGY M AIKAWA AUG 83 DAMD17-79-C-9029 1/1

UNCLASSIFIED F/G 6/13 NL

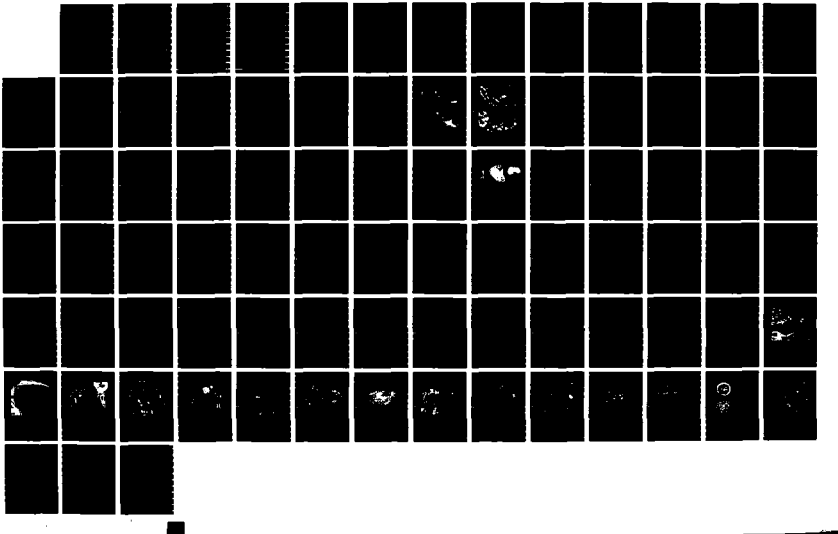

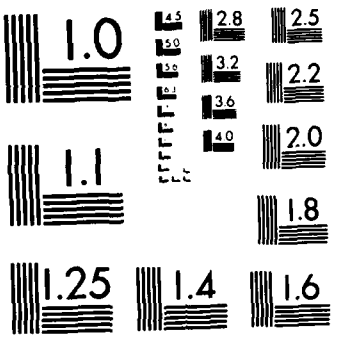

MICROCOPY RESOLUTION TEST CHART

AD_____

ELECTRON MICROSCOPY OF INTRACELLULAR PROTOZOA

ANNUAL REPORT

Masamichi Aikawa, M.D.
August, 1983

Supported by

U.S. Army Medical Research and Development Command

Fort Detrick, Frederick, MD. 21701-5012

Contract No. DAMD 17-79-C-9029

The Institute of Pathology

Case Western Reserve University

Cleveland, Ohio 44106

Approved for public release;
distribution unlimited

The findings in this report are not to be construed as an official Department of the Army position unless so designated by other authorized documents

10 AUG 1983

SECURITY CLASSIFICATION OF THIS PAGE (When Date Entered)

REPORT DOCUMENTATION PAGE	READ INSTRUCTIONS BEFORE COMPLETING FORM
1. REPORT NUMBER	2. GOVT ACCESSION NO. AD-A171635 / 3. RECIPIENT'S CATALOG NUMBER
4. TITLE (and Subtitle) Electron Microscopy of Intracellular Protozoa	5. TYPE OF REPORT & PERIOD COVERED Annual Report
	6. PERFORMING ORG. REPORT NUMBER
7. AUTHOR(s) Masamichi Aikawa, M.D.	8. CONTRACT OR GRANT NUMBER(s) DAMD17-79-C-9029
9. PERFORMING ORGANIZATION NAME AND ADDRESS Case Western Reserve University Cleveland, Ohio 44106	10. PROGRAM ELEMENT, PROJECT, TASK AREA & WORK UNIT NUMBERS
11. CONTROLLING OFFICE NAME AND ADDRESS U.S. Army Medical Research & Development Command, Fort Detrick, Frederick, MD 21701	12. REPORT DATE August, 1983
	13. NUMBER OF PAGES
14. MONITORING AGENCY NAME & ADDRESS (if different from Controlling Office)	15. SECURITY CLASS. (of this report) Unclassified
	15a. DECLASSIFICATION/DOWNGRADING SCHEDULE

16. DISTRIBUTION STATEMENT (of this Report)

Approved for public release; distribution unlimited.

17. DISTRIBUTION STATEMENT (of the abstract entered in Block 20, if different from Report)

18. SUPPLEMENTARY NOTES

19. KEY WORDS (Continue on reverse side if necessary and identify by block number)

20. ABSTRACT (Continue on reverse side if necessary and identify by block number)

Summary

During this fiscal year, in collaboration with LTC Berman and his associates, we studied the morphological effects of an anti-trypanosomal drug, WR 163577 on Trypanosoma rhodesiense by electron microscopy. Exposure of trypomastigotes to a low concentration of the drug resulted only in condensation of kinetoplast DNA fibrils. Exposure to higher drug

DD FORM 1 JAN 73 1473 EDITION OF 1 NOV 65 IS OBSOLETE

SECURITY CLASSIFICATION OF THIS PAGE (When Date Entered)

concentrations caused clumping of nuclear chromatin and of cytoplasmic contents. Although alteration of kinetoplast DNA is the first detectable drug-induced change, the function of the kinetoplast in mammalian forms of African Trypanosomes is unclear, and the secondary changes in the nucleus and cytoplasm may constitute the functionally significant alterations caused by WR 163577.

We also performed an experiment on ultrastructural localization of protective antigens of Plasmodium yoelii by the use of monoclonal antibodies and ultrathin cryomicrotomy. Freeman et al. reported the production of two hybridoma cell lines secreting monoclonal antibodies (25.77 and 25.1), both of which react specifically with erythrocytic merozoites of P. yoelii in the indirect immunofluorescence assay. Antibody 25.77 was reactive with a localized region within each merozoite, while antibody 25.1 appeared to be specific for the membrane of schizonts and merozoites. Both antigens induced protective immunity in mice against P. yoelii. In order to establish the precise localization of these protective antigens within erythrocytic merozoites, ultrathin cryomicrotomy was used in conjunction with the monoclonal antibodies and protein A-gold. Our results showed that gold particles were exclusively concentrated over the rhoptries when erythrocytic merozoites were incubated with antibody 25.77. On the other hand, gold particles were distributed uniformly over the merozoite surface when parasites were incubated with antibody 25.1. These results demonstrated, for the first time, that a protective antigen of the erythrocytic stage of P. yoelii is localized within the rhoptries.

In addition, we studied the ultrastructure of the sexual stages of P. gallinaceum during gametogenesis, fertilization, and early zygote transformation. New observations were made regarding the parasitophorous vacuole (PV) of gametocytes and the process of emergence in male and female gametocytes. Whereas, female gametocytes readily disrupted both the PV membrane and host cell plasmalemma during emergence, male gametocytes frequently failed to break down the plasmalemma of the host cell. Following fertilization, the male nucleus appeared to travel through a channel of endoplasmic reticulum in the female gamete before fusing with the female nucleus at a region in which the nuclear envelope is thrown into extrusive convoluted folds. Polarization of the zygote nucleus, in association with the appearance of a perinuclear spindle of cytoplasmic microtubules, preceded all other changes in the developing zygote. After nuclear polarization becomes apparent, electron dense material is deposited beneath the zygote pellicle and a canopy is formed, which eventually extended over the entire apical end of the developing ookinete.

Summary

During this fiscal year, in collaboration with LTC Berman and his associates, we studied the morphological effects of an anti-trypanosomal drug, WR 163577 on Trypanosoma rhodesiense by electron microscopy. Exposure of trypomastigotes to a low concentration of the drug resulted only in condensation of kinetoplast DNA fibrils. Exposure to higher drug concentrations caused clumping of nuclear chromatin and of cytoplasmic contents. Although alteration of kinetoplast DNA is the first detectable drug-induced change, the function of the kinetoplast in mammalian forms of African Trypanosomes is unclear, and the secondary changes in the nucleus and cytoplasm may constitute the functionally significant alterations caused by WR 163577.

We also performed an experiment on ultrastructural localization of protective antigens of Plasmodium yoelii by the use of monoclonal antibodies and ultrathin cryomicrotomy. Freeman et al. reported the production of two hybridoma cell lines secreting monoclonal antibodies (25.77 and 25.1), both of which react specifically with erythrocytic merozoites of P. yoelii in the indirect immunofluorescence assay. Antibody 25.77 was reactive with a localized region within each merozoite, while antibody 25.1 appeared to be specific for the membrane of schizonts and merozoites. Both antigens induced protective immunity in mice against P. yoelii. In order to establish the precise localization of these protective antigens within erythrocytic merozoites, ultrathin cryomicrotomy was used in conjunction with the monoclonal antibodies and protein A-gold. Our results showed that gold particles were exclusively concentrated over the rhoptries when erythrocytic merozoites were incubated with antibody 25.77. On the other hand, gold particles were distributed uniformly over the merozoite surface when parasites were incubated with antibody 25.1. These results

demonstrated, for the first time, that a protective antigen of the erythrocytic stage of P. yoelii is localized within the rhoptries.

In addition, we studied the ultrastructure of the sexual stages of P. gallinaceum during gametogenesis, fertilization, and early zygote transformation. New observations were made regarding the parasitophorous vacuole (PV) of gametocytes and the process of emergence in male and female gametocytes. Whereas, female gametocytes readily disrupted both the PV membrane and host cell plasmalemma during emergence, male gametocytes frequently failed to break down the plasmalemma of the host cell. Following fertilization, the male nucleus appeared to travel through a channel of endoplasmic reticulum in the female gamete before fusing with the female nucleus at a region in which the nuclear envelope is thrown into extrusive convoluted folds. Polarization of the zygote nucleus, in association with the appearance of a perinuclear spindle of cytoplasmic microtubules, preceded all other changes in the developing zygote. After nuclear polarization becomes apparent, electron dense material is deposited beneath the zygote pellicle and a canopy is formed, which eventually extended over the entire apical end of the developing ookinete.

Forward

In conducting the research described in this report, the investigators adhered to the Guide for Laboratory Animal Facilities and Care, as promulgated by The Committee on The Guide for Laboratory Animal Resources, National Academy of Science - National Research Council.

Table of Contents

Detailed Report

a) Fine structural alterations in Trypanosoma rhodesiense treated with the prophylactic drug WR 163577 in vitro.

b) Ultrastructural localization of protective antigens of Plasmodium yoelii by the use of monoclonal antibodies and ultrathin cryomicrotomy.

c) Ultrastructural observations on gametogenesis, fertilization, and zygote formation of the avian malarial parasite. Plasmodium gallinaceum.

Title: Fine Structural Alterations in *Trypanosoma rhodesiense* treated with WR 163577 *in vitro*.

Authors: Berman, J.D., *
Oka,M. **
Aikawa, M. **

Institutions:

*Dept. of Parasitology
Div., Experimental Therapeutics
Walter Reed Institute of Research
Washington, D.C. 20307

**Dept. of Pathology
Case-Western Reserve University
Cleveland, Ohio

Abstract

Fine-structural alterations in Trypanosoma rhodesiense trypomastigotes exposed to WR 163577, a prophylactic agent against animal African trypanosomiasis, were determined in vitro. Exposure of trypomastigotes to a low concentration of drug resulted only in condensation of kinetoplast DNA fibrils. Exposure to higher drug concentrations caused clumping of nuclear chromatin and of cytoplasmic contents. Although alteration of kinetoplast DNA is the first detectible drug-induced change, the function of the kinetoplast in mammalian forms of African trypanosomes is unclear, and the secondary changes in the nucleus and cytoplasm may constitute the functionally significant alterations caused by WR 163577.

Introduction

Williamson commented in 1976 that "the simple and distressing fact [is] that no new effective drugs for [African] trypanosomiasis, human or animal, have been brought into field use for 20 years." (6) In 1978,Kinnamon and Rane reported that 1,6-bis(6-amino-2-methyl-4-quinolylamino) hexane (WR 163577) protected mice when challenged with the Wellcome CT strain of Trypanosoma rhodesiense up to 10 months after drug administration (2). The potential of WR 163577 to protect animals for approximately a year after single dosing makes it a prime candidate for a prophylactic agent against trypanosmiasis in Africa, where field conditions preclude frequent visits to veterinary stations.

The mechanism of action of WR 163577 has not been determined. We here report fine-structural observations on the effect of WR 163577 on T.rhodesiense bloodstream forms in vitro.

Materials and Methods

Trypomastigotes of the Wellcome CT strain of T.rhodesiense were obtained from the blood of inoculated rats as previously described(1). A stock solution of WR 163577 dinitrate(Walter Reed Institute of Research drug inventory) was made by dissolving 25 mg drug in 1 ml dimethylsulfoxide(DMSO),and was diluted with parasite incubation medium (1) before use. The antitrypanosomal activity of WR 163577 in vitro was quantitated by the inhibition of incorporation of radiolabelled thymidine and leucine into macromolecules of parasites exposed to 1-100 μ g drug/ml,precisely as described by Casero et al.(1).

For electron microscopy, 50 x 10^6 organisms in 5 ml of incubation medium (1) were treated with 10 μl DMSO(control cultures)or 5-500 μg diluted drug(experimental cultures). After 2 hours of incubation (37°C, 5% CO_2), the number and motility of organisms in 0.1 mm^3 of each culture was determined in a hemocytometer. The rest of each culture was centrifuged (1000 x g x 15', RT). The pellets containing the parasites were resuspended in 0.1 of incubation medium to which was added 1.0 ml of fixative(0.1 M cacodylate (pH=7.4) containing 2% glutaraldehyde and 4% sucrose). After being fixed for 1 hr at room temperature, the parasites were washed three times by centrifugation with 0.1 M cacodylate containing 4% sucrose. The washed parasites were postfixed in 1% osmium tetroxide for 1 h.,dehydrated in an ascending concentration of alcohol, and embedded in Spurr's medium. The resulting blocks were cut with a Porter-Blum MT-2 ultramicrotome. Thin sections on copper grids were stained with 1% uranyl acetate and lead citrate, and were examined with a JEOL 100 CX electron microscope.

Results

Antitrypanosomal activity of WR 163577 in vitro

The incorporation of radiolabelled macromolecular presursors into Trypanosoma rhodesiense trypomastigotes over 3 hours was 50% inhibited by a drug concentration of 3 μg/ml,and was 85% inhibited by 10 μg drug/ml. Fine-structural observations were therefore performed on organisms treated for 2 hours with 0(controls), 1, 10 and 100 μg drug/ml. At the end of the 2 hour incubation period, control organisms were present at a concentration of 12 x 10^6/ml and were viable by the criterion of vigorous motility. Although 12 x 10^6 organisms were present in all WR 163577-treated cultures, the increased activity of higher drug concentrations was apparent by observation of motility. Organisms exposed to 1 μg/ml were as vigorously motile as controls; organisms exposed to 10 μg/ml were moderately motile; and organisms exposed to 100 μg/ml were barely motile.

Fine-structural observations

Control organisms demonstrated a nucleus with a nucleolus, a prominent Golgi complex, a flagellum with a flagellar pocket, ribosomes and endoplasmic reticulum, and many vesicles and osmiophilic granules(figure 1). The kinetoplast DNA of the kinetoplast-mitochondrion is located posterior to the nucleus and consists of several well-arranged double rows of fibrils lying parallel to each other(figure 1).

Parasites treated with 1 μg WR 163577/ml were intact except for the DNA of the kinetoplast. Instead of being well arranged, the DNA fibrils were partially clumped together to form electron dense granules(figure 2). Organisms exposed to 10 μg drug/ml demonstrated further clumping of the kinetoplast DNA, and an increased electron density of the mitochondrial

matrix(figure 3). In addition,exposure to this drug concentration resulted in changes to organelles other than the kinetoplast-mitochondrion. Clumping of chromatin was observed along the nuclear membrane and in the nuclear matrix, and scattered electron dense granules became apparent in the cytoplasm(figure 3).

In parasites exposed to 100 μg drug/ml, the aforementioned clumping of kinetoplast DNA and of nuclear chromatin, formation of electron dense cytoplasmic granules, and swelling of the parasites became exacerbated(figure 4). Also,treatment with this dosage of drug resulted in swollen, irregularly shaped mitochrondria (fig. 4).

Discussion

The *in vivo* prophylactic agent WR 163577 demonstrated *in vitro* activity against *Trypanosoma rhodesiense* trypomastigotes. Parasite motility and macromolecular synthesis were unchanged or slightly altered in organisms exposed to 1 μg drug/ml, but were partially or completely suppressed in organisms exposed to 10 and 100 μg drug/ml. In organisms treated with 1 μg/ml, the only discernable fine-structural alteration was clumping of the kinetoplast DNA fibrils. Exposure to the higher drug concentrations resulted in clumping of nuclear chromatin and of cytoplasmic material in addition to kinetoplast-mitochondrial changes. Condensation of kinetoplast DNA is therefore the primary fine-structural mechanism of WR 163577, and condensation of nuclear nucleic acid and cytoplasmic material are the secondary mechanisms.

In solution, the base of WR 163577 dinitrate is a positively charged cation, as are the bases of the classical antitrypanomonal agents pentamidine, hydroxystilbamidine, and Berenil(diamidines), Ethidium(an aminophenanthridine), and Antrycide(an aminoquinaldine). The initial morphologic change in *T.rhodesiense* exposed to each of these latter five agents is condensation of kinetoplast DNA(3,5). Pentamidine additionally produces a reduction in ribosomal density(3) and segregation of the nucleolus into dark and light masses(5). Because interaction of cationic drugs with nucleic acids is reasonable, and because all the drugs initially alter kinetoplast DNA, it is tempting to ascribe their activity to derangement of kinetoplast DNA function. However, the function of the kinetoplast and its DNA is not well described. Furthermore, there are naturally dyskinetoplastic trypanosomes in which the kinetoplast DNA is represented by a fibrous knot(4), but which are pathogenic to mammals(5). Such considerations led Williamson to conclude that condensation of kinetoplast DNA is unlikely to be the mechanism

of activity for the 5 classical agents(5). Similarly, the striking changes in the kinetoplast DNA produced by WR 163577 may only be functionally significant if that organelle is found to be necessary for mammallian pathogenicity. In the light of present knowledge, it may be hypothesized that the secondary alterations in the parasite--clumping of nuclear nucleic acid and of cytoplasmic components--are likely to be the morphologic mechanisms for this antitrypanosomal agent.

Figure Legends

Figure 1: Electron micrograph of non-drug treated T. rhodesiense trypomastigotes (control). The nucleus (N), nucleolus (n), kinetoplast DNA (KD), flagellum (F), ribosomes, and sub-pellicular microtubules (Mt) are easily seen. X20,000. Inset: A high magnification micrograph showing a kinetoplast with well-arranged rows of DNA fibrils. X48,000.

Figure 2: Electron micrograph of T. rhodesiense exposed to 1 μg of WR 163577/ml. The nucleus (N) and cytoplasm are unaltered with the exception of the kinetoplast (See inset). X21,000. Inset: A kinetoplast at higher power, demonstrating partial clumping of its DNA. X58,000.

Figure 3: Electron micrograph of T. rhodesiense exposed to 10 μg of WR 163577/ml. Marked clumping of nuclear chromatin (C) and of cytoplasmic contents in addition to condensed kinetoplast DNA (arrow) is seen. Decreased density of cytosol also is apparent. X30,000.

Figure 4: Electron micrograph of T. rhodesiense exposed to 100 μg of WR 163577/ml. Exacerbation of changes-- such as condensation of kinetoplast DNA (arrow), clumping of nuclear chromatin (N), and a decrease in density of the cytosol with scattered, electron-dense granular material (G)-- is evident. X58,000.

Acknowledgement:

We thank Mr. Harold(Dexter) Fairbanks and Dr. Chris Lambros for assistance in the determinaton of the antitrypanosomal activity of WR 163577.This work was supported in part by research grants from the U.S.Army Research and Development Command(# DAMD 17-79C-9029) and U.S.P.H.S.(# AI 15351) to M.A.

Literature Cited

(1) Casero, R.A., Klayman, D.L., Childs, G.E., Scoville, J.P., and Desjardins, R.E. 1980. Activity of 2-acetylpyridine thiosemicarbazones against Trypanosoma rhodesiense in vitro. Antimicrob. Agents Chemotherapy 18 317-322.

(2) Kinnamon,K.E. and Rane ,D.S. 1978. Greater than 1 year protection of mice from lethal Trypanosoma rhodesiense infections by prophylactic drugs and immunity. Int. J. Parasitol. 8 515-523.

(3) Macadam, R.F., and Williamson, J. 1972. Drug effects on the fine structure of Trypanosoma rhodesiense: diamidines. Trans. Roy. Soc. Trop. Med. Hyg. 66 897-904.

(4) Vickerman,K. 1970. Ultrastructure of Trypanosoma and relation to function. in The African Trypanosomes. Ed. H.W. Mulligan. pp 60-66. Wiley,N.Y.

(5) Williamson, J., Macadam, R.F., and Dixon, H. 1975. Drug-induced lesions in trypanosome fine structure: a guide to modes of trypanocidal action. Biochem. Pharmacol 24 147-151.

(6) Williamson,J. 1976. Chemotherapy of African trypansomiasis. Trop. Dis.Bull. 73 531-542.

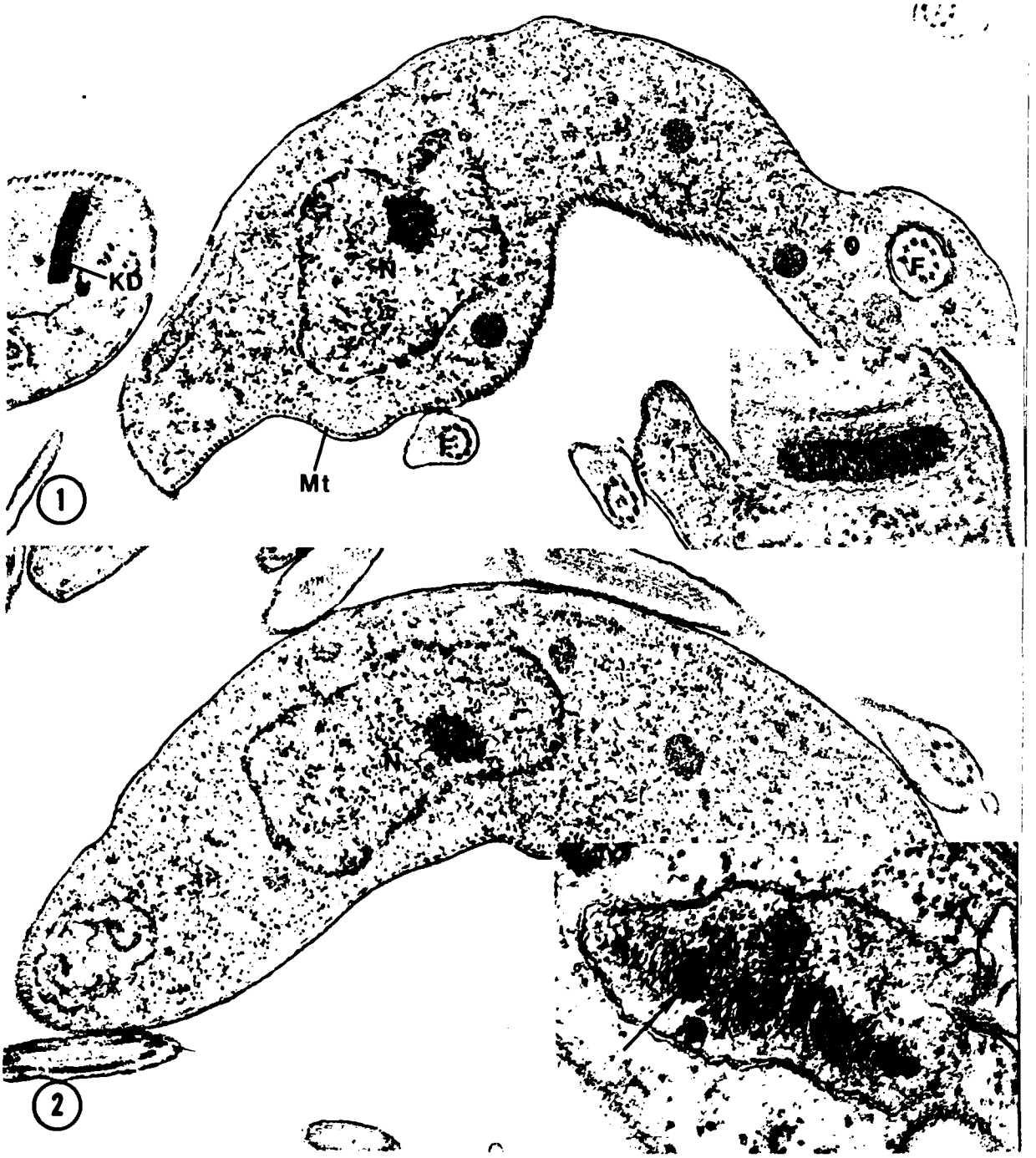
KD
N
F
Mt
E
1
N
2

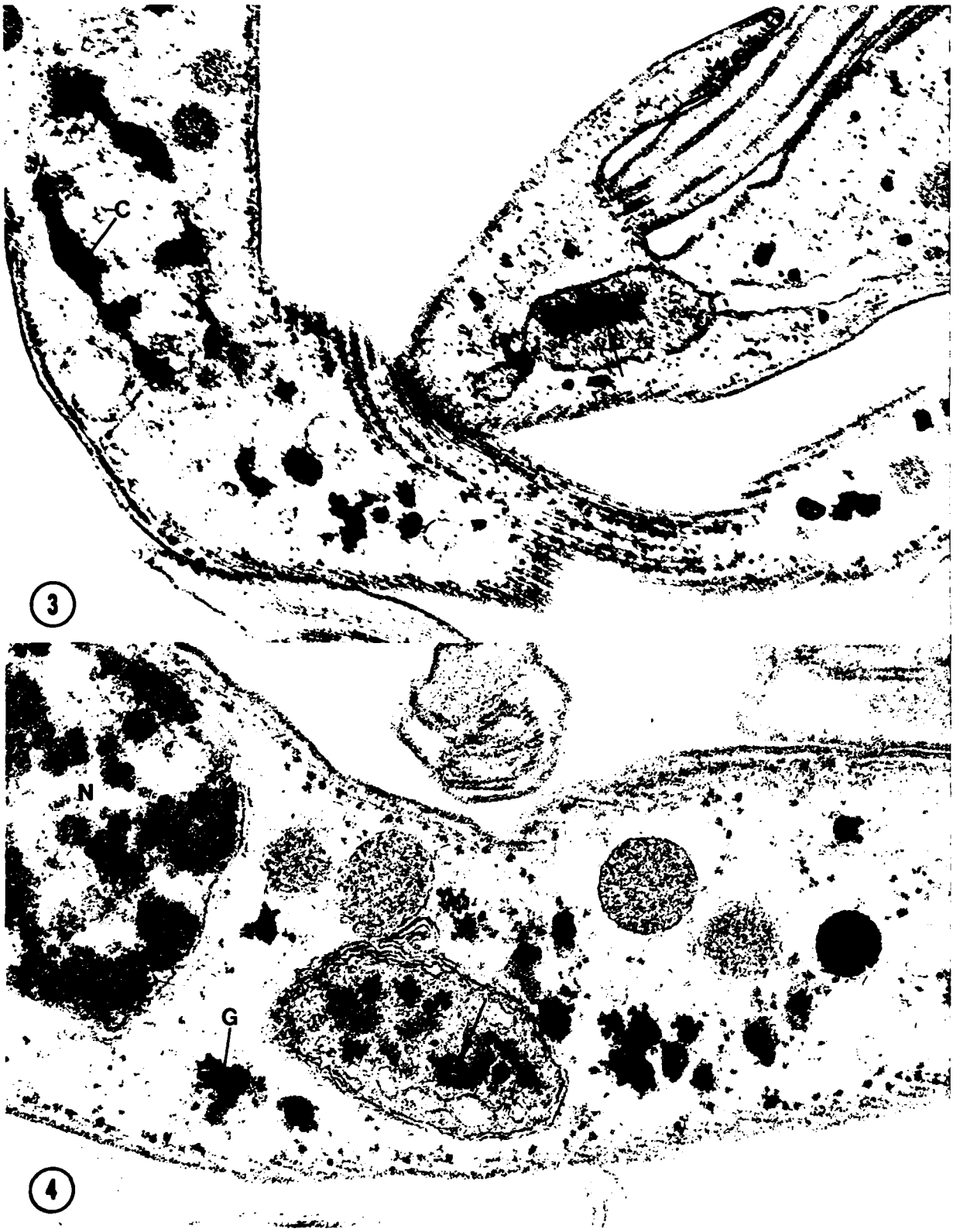
C
3
N
G
4

ULTRASTRUCTURAL LOCALIZATION OF PROTECTIVE ANTIGENS OF *PLASMODIUM YOELII* BY THE USE OF MONOCLONAL ANTIBODIES AND ULTRATHIN CRYOMICROTOMY[1]

Running Title: Localization of Protective Antigens of *Plasmodium*

Mikio Oka[*], Masamichi Aikawa[2*]

Robert R. Freeman[†], and Anthony A. Holder[†]

*Institute of Pathology, Case Western Reserve University,

Cleveland, Ohio 44106, USA

and

[†]Department of Molecular Biology, The Wellcome Research Laboratories,

Beckenham, Kent BR3 3BS, England

Footnotes

[1]This work was, in part, supported by research grants from USPHS (AI-10645), the U.S. Army R&D Command (DAMD17-79C-9029), and the World Health Organization (T16/181/M2/52).

[2]Correspondence should be addressed to Dr. M. Aikawa, Institute of Pathology, Case Western Reserve University, Cleveland, Ohio 44106

Clinical and naturally acquired immunity to malaria is directed mainly against the asexual erythrocytic stage and protective antibodies against this stage are of importance in elimination of the parasites. It has been suggested that the protective antibodies act against either mature schizonts or extracellular merozoites (1, 2). Recently, Holder and Freeman reported (3) that two protective protein antigens of 230,000 and 235,000 molecular weight (MW) are associated with the erythrocytic stage of *Plasmodium yoelii* and can be purified using monoclonal antibodies. The 230,000 MW antigen was recognized by antibody 25.1 and the 235,000 MW antigen was recognized by antibody 25.77. In the indirect immunofluorescence assay, antibody 25.1 appeared to react specifically with schizont membrane and the surface of the erythrocyte merozoite, whereas antibody 25.77 appeared to react with a localized region within the merozoite.

In order to determine the ultrastructural localization of these protective antigens, frozen sections of the erythrocytic parasites prepared by cryoultramicrotomy (4, 5) were reacted with the monoclonal antibodies and then the binding sites of the antibodies were visualized by formation of protein A-gold complexes (6).

Our data showed that the 230,000 MW antigen, or a fragment of it, recognized by antibody 25.1 is distributed over the surface of merozoites and that the 235,000 MW antigen, recognized by the antibody 25.77 is located within the rhoptries of merozoites.

MATERIALS AND METHODS

Virulent *P. yoelii* (17XL strain) was maintained either as a frozen stabilate at -70°C or by repeated blood passage through BALB/c mice. Parasitized erythrocytes were collected in heparinized 0.1M phosphate buffered saline (PBS), at pH 7.3. After washing with PBS, the erythrocytes were fixed with

1% formaldehyde containing 0.2% glutaraldehyde in PBS for 10 min. at 4°C and stored in PBS until used. An aliquot of unfixed-erythrocytes was lysed with 0.013% saponin to prepare free forms of the erythrocytic stages of the parasites (7).

Monoclonal antibodies 25.1 and 25.77 were purified by protein A-Sepharose chromatography from ascites fluids of mice carrying the hybridomas WIC 25.1 and WIC 25.77, as described previously (3).

For visualization of bound antibodies, colloidal gold particles were prepared by reducing $HAUCL_4$ with sodium ascorbate, according to the method of Horrisberger (8). The particles were absorbed with Staphylococcal protein A (Pharmacia Fine Chemicals, Sweden) to prepare a stabilized suspension of protein A-gold complexes (6). The preparation was pelleted to remove excess protein A at 50,000g for 45 min. The pellet was then suspended in PBS containing 0.05% carbowax (MW 20,000) and centrifuged in a 10-30% continuous glycerol gradient at 48,000g for 30 min. to select homogeneous sized particle fractions. The fractions were dialyzed against 0.01M PBS overnight and stored at 4°C.

The fixed erythrocytes were embedded in 30% bovine serum albumin (BSA) cross-linked with 0.5% glutaraldehyde for 30 min. at room temperature. The gel was incubated in 1.3M sucrose for 60 min. and frozen in liquid nitrogen. Frozen thin sections were cut by cryoultramicrotomy at -90°C (4) and picked up with a wire loop filled with 2.3M sucrose in PBS. They were then transferred to a carbon coated formvar grid, freshly cleaned in an ion glow discharge, and then washed in phosphate buffered saline containing 0.01M glycine (PBS +G).

The sections on grids were floated, sections down, on a drop of a solution containing monoclonal antibody 25.1 (330 μg/ml) or 25.77 (200 μg/ml) diluted with PBS + G for 60 min. at room temperature. After washing in PBS + G,

they were then put on a drop of protein A-gold solution in PBS + G, containing 1% BSA for 60 min. at room temperature, followed by washing in PBS + G. The sections were then fixed with 0.5% glutaraldehyde in PBS and rinsed in distilled water. After staining with 0.5% osmium, 1% neutral uranyl acetate, 3% acidic uranyl acetate, and 1% lead citrate, sections were finally embedded in the mixture of 0.8% methycellulose and 0.3% polyethylene glycol (MW 1540) in distilled water.

Unfixed erythrocytes, treated with 0.013% saponin, were incubated with the antibody 25.1. After washing with the culture medium 199, they were incubated with protein A-gold for 60 min. and then washed and fixed with 0.5% glutaraldehyde. Finally, the suspension of erythrocytes was processed for electron microscopy. In order to demonstrate the specificity of the labeling, the following controls were performed: 1) IgG from normal mouse serum was used instead of monoclonal antibodies. 2) The preparations were incubated with protein A-gold alone.

RESULTS AND DISCUSSION

Immunocytochemical labeling of frozen sections of the erythrocytic stages of *P. yoelii*, incubated with antibody 25.1, showed the binding of gold particles to the plasma membrane of each merozoite (Fig. 1). No specific binding of gold particles was found on the membrane of other erythrocytic stages of the parasite. When extracellular mature schizonts and/or merozoites, prepared by lysing the parasitized erythrocytes with saponin, were incubated with antibody 25.1, gold particles were clearly bound to the surface of parasites (Fig. 2). After incubation of thin sectioned *P. yoelii* erythrocytic stages with antibody 25.77, gold particles were specifically bound to electron-dense rhoptries, which are located at the apical end of the merozoite (Fig. 3). When IgG from normal mouse serum was used instead of the monoclonal antibodies, no gold particles were associated with the parasites. Similarly, protein A-gold did not bind to the parasites incubated with protein A-gold alone.

Monoclonal antibody 25.1, which recognized a 230,000 MW antigen of the erythrocytic stages of *P. yoelii* and a series of processing fragments derived from it, was reported to react with the surface of the merozoite in the indirect immunofluroescence assay. Our results confirm that the 230,000 MW antigen is present on the parasite plasma membrane of schizonts and merozoites. It has been suggested that antibodies against the surface antigens of merozoites are important for the elimination of parasites. These antibodies may inhibit merozoite invasion of the erythrocyte and may facilitate phagocytic ingestion of the parasites by macrophages (9, 10). Recently, it has been reported that an inhibitory monoclonal antibody reacts with a 230,000 MW antigen over the surface of merozoites of the monkey malaria parasite, *P. knowlesi* (11). Although the antibody 25.1 was not effective against *P. yoelii* infection on passive transfer (12), mice immunized with the 230,000 MW *P. yoelii* antigen were protected against a challenge with *P. yoelii.* Thus, the humoral immune response to the 230,000 MW antigen may not be enough to establish protective immunity to *P. yoelii* infection. It is well known that not only B cells, but also T cells play key roles in the development of protective immunity to malaria. Animals, depleted of T cells, are unable to control parasitemia satisfactorily (13). Alternatively, antibody 25.1 may react with a determinant on the 230,000 MW protein, which is different from the determinants concerned with the induction of protective immunity.

Monoclonal antibody 25.77, which recognized the 235,000 MW antigen, was reported to react specifically with a localized region within the merozoite by indirect immunofluorescence. Antibody 25.77 was protective on passive transfer (12), and mice immunized with the purified 235,000 MW antigen were successfully protected against *P. yoelii* infection (3). Our results demonstrate the localization of the 235,000 MW antigen within the rhoptries of *P. yoelii* merozoites. A ductule runs from the rhoptries to the apical end of the merozoite, which is the contact point of the merozoite and the membrane of the erythrocyte during invasion.

This ductule is thought to release the rhoptry contents from the apical end on to the erythrocyte membrane (14, 15), and it has been suggested that rhoptry contents may be concerned with merozoite entry into erythrocytes (16). Therefore, the 235,000 MW antigen, localized in the rhoptries, may play an important role during invasion of *P. yoelii* merozoites into erythrocytes, and antibody 25.77 may inhibit invasion by inactivating the function of rhoptries or of the rhoptry contents.

Acknowledgment

We gratefully acknowledge the excellent technical assistance of Mr. C. L. Hsieh and Ms. Ana Milosavljevic. We would also like to thank Drs. R. Nussenzweig, I. Ivanoff, D. Sabatini, A. Schwartz, and G. Cross for their helpful suggestions.

References

1. Freeman, R. R., and C. R. Parish. 1981. *Plasmodium yoelii:* Antibody and the maintenance of immunity in BALB/c mice. Exp. Parasitol. 52:18.
2. Diggs, C., and A. Osler. 1975. Humoral immunity in rodent malaria III: Studies on the site of antibody action. J. Immunol. 114:1243.
3. Holder, A. A.,and R. R. Freeman. 1981. Immunization against blood-stage rodent malaria using purified parasite antigens. Nature 294:361.
4. Geuze, J. J., J. W. Slot, and K. T. Tokuyasu. 1979. Immunocytochemical localization of amylase and chymotrypsinogen in the exocrine pancreatic cell with special attention to the Golgi complex. J. Cell. Biol. 82:697.
5. Rindler, M. J., I. E. Ivanov, E. Rodriguez-Boulan, and D. D. Sabatini. 1981. Simultaneous budding of virus with opposite polarity from doubly infected MDCK cells. J. Cell. Biol. 91:118a.
6. Romano, E. L., and M. Romano. 1977. Staphylococcal protein A bound to colloidal gold: A useful reagent to label antigen-antibody sites in electron microscopy. Immunochemistry 14:711.
7. Zuckerman, A., D. Spira, and J. Hamburger. 1967. A procedure of the harvesting of mammalian plasmodia. Bull. W.H.O. 37:431.
8. Horrisberger, M., and J. Rosset. 1977. Colloidal gold, a useful marker of transmission and scanning electron microscopy. J. Histochem. Cytochem. 25:295.
9. Miller, L. H., M. Aikawa, and J. A. Dvorak. 1975. Malaria (*Plasmodium knowlesi)* merozoites: Immunity and the surface coat. J. Immunol. 114:1237.
10. Brooks, C. B., and J. P. Kreier. 1978. Role of surface coat on *in vitro* attachment and phagocytosis of *Plasmodium berghei* by peritoneal macrophages. Infect. Immunol. 20:927.

11. Epstein, N., L. H. Miller, D. C. Kaushel, I. J. Udeinya, J. Rener, R. L. Howard, R. Asofsky, M. Aikawa, and R. L. Hess. 1981. Monoclonal antibodies against a specific surface determinant on malarial *(Plasmodium knowlesi)* merozoites block erythrocyte invasion. J. Immunol. 127:212.

12. Freeman, R. R., A. J. Trejdosiewicz, and G. A. M. Cross. 1980. Protective monoclonal antibodies recognizing stage-specific merozoite antigens of a rodent malaria parasite. Nature 284:366.

13. Jayawardena, A. N., G. A. T. Targett, R. L. Carter, E. Leucharo, and A. J. S. Davies. 1977. The immunological response of CBA mice to *P. yoelii* 1. General characteristics: The effects of T-cell deprivation and reconstitution with thymus grafts. Immunology 32:849.

14. Ladda, R. L., M. Aikawa, and H. Sprinz. 1969. Penetration of erythrocytes by merozoites of mammalian and avian malarial parasites. J. Parasitol. 55:633.

15. Aikawa, M., L. H. Miller, J. Johnson, and J. Rabbege. 1978. Erythrocyte entry by malarial parasites: a moving junction between erythrocyte and parasite: J. Cell Biol. 77:72.

16. Kilejian, A. 1976. Does a histidine-rich protein from *Plasmodium lophurae* have a function in merozoite penetration? J. Protozool. 23:272.

Figure Legends

Fig. 1. Electron micrograph of a cryosectioned *P. yoelii* merozoite (M) reacted with antibody 25.1 and followed by protein A-gold label. Gold particles (arrow) bind to the plasma membrane of the parasite. X98,000

Fig. 2. Electron micrograph of an epoxy embedded and thin sectioned extracellular merozoite (M) after saponin treatment. The parasite was reacted with antibody 25.1 and followed by protein A-gold label. Gold particles (arrow) are seen along the parasite's plasma membrane. Note an electron-dense membrane bound rhoptry (R) in the merozoite. X57,000

Fig. 3. Electron micrograph of a cryosectioned *P. yoelii* merozoite (M) which was reacted with antibody 25.77 and followed by protein A-gold label. Gold particles (arrow) bind specifically to rhoptries (R). X62,000

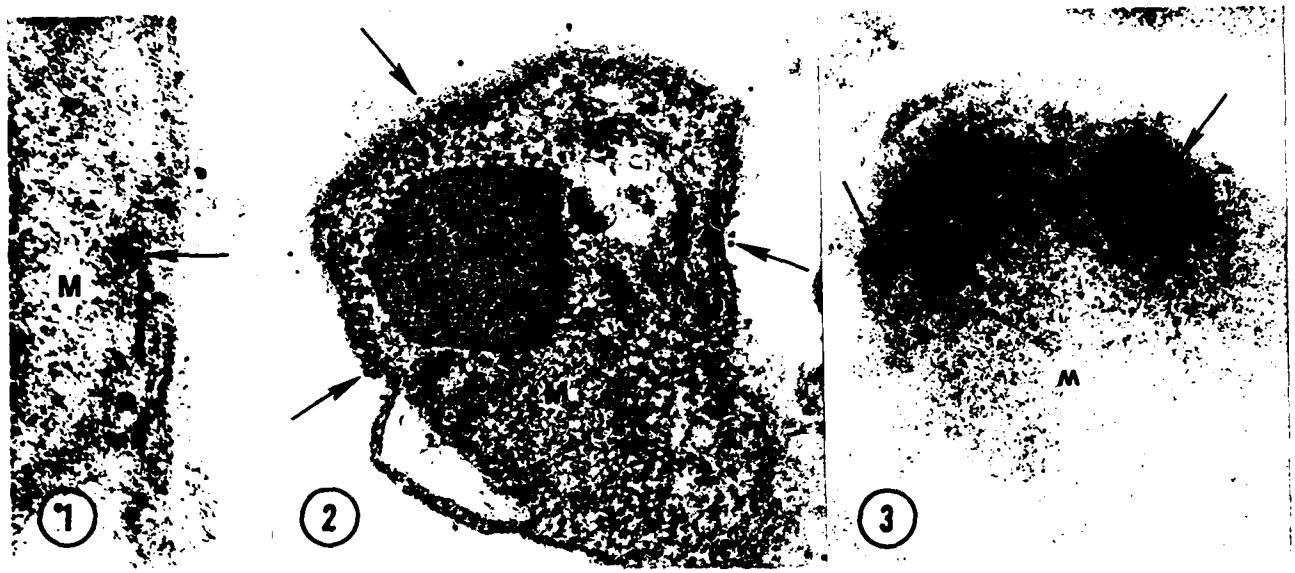
M
1
2
M
3

New observations on gametogenesis, fertilization and zygote transformation in *Plasmodium gallinaceum*

Masamichi Aikawa†, Richard Carter*,
Yoshihiro Ito†[1], and Mary M. Nijhout*[2]

†Institute of Pathology, Case Western Reserve University,
Cleveland, Ohio 44106
and
*Laboratory of Parasitic Diseases,
National Institute of Allergy and Infectious Diseases,
Bethesda, Maryland 20205

Current address [1]The Department of Parasitology, The University of Tokushima, Tokushima, Japan.

[2]Department of Zoology, Duke University, Durham, North Carolina.

Address Correspondence to:
Masamichi Aikawa, M.D.
Institute of Pathology
Case Western Reserve University
Cleveland, Ohio 44106

Running Title: Gametogenesis and zygote transformation of *P. gallinaceum*

ACKNOWLEDGMENTS

We gratefully acknowledge the excellent technical assistance of Mr. M. Oka, Ms. Cynthia A. Grotendorst and Ms. Ana Milosavljevic. This paper was partially supported by research grants from USPHS (AI-10645) and from the U.S. Army R & D Command (DAMD 17-79C-9029). This is contribution No. to the Army Research program on antiparasitic drugs.

SYNOPSIS

The ultrastructure of the sexual stages of *Plasmodium gallinaceum* during gametogenesis, fertilization, and early zygote transformation are described. New observations are made regarding the parasitophorous vacuole (PV) of gametocytes and the process of emergence in male and female gametocytes. Whereas female gametocytes readily disrupted both the PV membrane and host cell plasmalemma during emergence, male gametocytes frequently failed to break down the plasmalemma of the host cell. New observations and hypothesis are presented on the behavior of the male gamete nucleus. Following fertilization, the male nucleus appears to travel through a channel of endoplasmic reticulum in the female gemete before fusing with the female nucleus at a region in which the nuclear envelope is thrown into extensive convoluted folds.

Polarization of the zygote nucleus, in association with the appearance of a perinuclear spindle of cytoplasmic microtubules, preceded all other changes in the developing zygote. After nuclear polarization becomes apparent, electron dense material is deposited beneath the zygote pellicle, and a canopy is formed, which eventually extends over the entire apical end of the developing ookinete. As the apical end begins to extend outward, polar rings, micronemes, and subpellicular microtubules become visible in this portion and a "virus-like" inclusion known as a crystalloid is formed in the posterior portion of the zygote.

When female gametes are prevented from being fertilized, the cytoplasm at 24 hours after gametogenesis is devoidof most of those organelles found in the developing zygote or the mature ookinete. The cell is surrounded only by a single membrane. Although at various points beneath the membrane there are deposits of electron dense material reminiscent of those deposited in the zygote, no further development of ookinete structures takes place in the unfertilized female gamete.

INTRODUCTION

When malaria-infected blood is ingested by a mosquito, transformation of the malarial gametocytes to gametes is initiated, and fertilization of female by male gametes takes place in the lumen of the mosquito midgut. The resultant zygotes differentiate in the course of about 24 hours into motile ookinetes which cross the mosquito midgut wall to become oocysts and eventually infected sporozoites in the salivary glands of the mosquito. The process of transformation of the gametocytes of malaria parasites and other Haemosporina into male and female gametes and subsequent fertilization have been described at an ultrastructural level for several species including the avian parasites, *Leucocytozoon* (3), *Haemoproteus* (16, 31), and *Parahaemoproteus* (13) and the mammalian malaria parasites, *Plasmodium yoelii nigeriensis* (30) and *P. falciparum* (29). Ultrastructural studies have also been reported on the morphology of the ookinete in various species of Haemosporina and its' transformation to the oocyst (5, 11, 18-20). The transformation of the zygote to ookinete has been described in some detail for *Haemoproteus columbae* (16, 17) but only to a limited extent in *Plasmodium* (24).

In the present study, we have examined the events from the initiation of gametogenesis to fertilization and the transformation of the zygote to the morphologically mature ookinete in the chicken malaria *Plasmodium gallinaceum*, a species now used extensively in the study of the sexual and mosquito midgut stages of malarial parasites (4, 21-23, 25-27). The development of methods for obtaining large numbers of purified gametes and zygotes of *P. gallinaceum* and the cultivation of these stages *in vitro* to mature and infective ookinetes has facilitated electron microscopic studies of the transformation of zygotes to ookinete in this species of malaria parasite (10,23). We have concentrated our studies here on aspects of these transformations not previously examined in detail. These aspects concern primarily the events associated with the

emergence of the gametocytes from the host cell during gametogenesis and the events associated with fertilization and early transformations in the zygote. We have also noted the ultrastructural development of female gametes which have not been fertilized but were otherwise grown under conditions which support the transformation of the zygotes to mature ookinetes (10).

MATERIALS AND METHODS

Parasitized blood from New Hampshire Red chickens infected with *P. gallinaceum* at a 50 to 60% parasitemia was drawn from the heart in a heparinized syringe and immediately diluted in 20 volumes of suspended activation (SA) solution (10 mM Tris, 166 mM NaCl and 10 mM glucose at pH 7.4) (26). In this solution, transformation of gametocytes into gametes is prevented. A sample of this material was immediately fixed for electron microscopy as described below.

The remainder of the preparation was resuspended in a gametogenesis activating solution (10 mM Tris, 166 mM NaCl, 10mM glucose, 25 mM $NaHCO_3$, pH 8.0 supplemented with 10% chicken serum). In this solution, gametogenesis is triggered immediately (26). Samples of the activated material were fixed for electron microscopy at intervals from 2 minutes to 2 hours after initiation. Zygotes of more than 2 hours post fertilization were purified as described by Kaushal et al. (23) and incubated under conditions supporting ookinete formation (10) in medium 199 supplemented with 2 mM L-glutamine 2.5 μg gentamycin/ml, 100 μg penicillin/ml 100 units insulin/ml and 1 unit streptomycin /ml at a zygote concentration of 2×10^6/ml. Preparations of unfertilized female gametes were obtained by diluting the cells in at least 200x their usual volume in a serum free solution immediately after initiating gametogenesis as described above. After 2 hours under these conditions, the male gametes were no longer capable of fertilizing the females, and the unfertilized female gametes were concentrated and purified and cultured in the same manner as the zygotes.

Samples of the parasites were fixed for electron microscopy at various times after initiating gametogenesis. All samples were fixed in 1.25% glutaraldehyde, 0.1 M Na cacodylate, 4% sucrose, pH 7.4, at room temperature for 1 hour. The samples were then washed in 0.1 M cacodylate buffer, pH 7.4, post-fixed in a 1% (w/v) OsO_4 solution in 0.1M cacodylate buffer and dehydrated in a descending series of alcohol and acetone. Samples were embedded in Spurr and the material sectioned with a diamond knife on a Porter-Blum MT-2 ultramicrotome, mounted on 200 mesh copper grids, stained with 1% uranyl acetate and lead citrate, and examined with a JEOL 100CX electron microscope.

RESULTS

Intracellular Gametocytes before Activation

Although the fine structure of the intracellular gametocytes of *P. gallinaceum* before activation and gametogenesis have been previously described (2, 32), it is necessary to review their basic structure in order to understand their subsequent transformations. Gametocytes of this species (Fig. 1) are surrounded by a pellicular complex, consisting of three sets of membranes. The outermost membrane represents the parasitophorous vacuole membrane (PVM) and the middle membrane is the plasmalemma of the gametocyte. The intervening space between these two membranes is thus the parasitophorous vacuole (PV). Unlike that of the trophozoites and schizonts, which is electron lucent (1, 2), the PV of the gametocytes of *P. gallinaceum* and other avain Haemospornia is of similar electron density to the cytoplasm of the host cell (2, 31), suggesting the possibility of significant functional differences between the PVM's of gametocytes and asexual parasites. The asexual trophozoites are distinguished from gametocytes by the absence of the third membrane beneath the parasite plasmalemma (1) which in the gametocytes consists of two closely opposed unit membranes entirely surrounding the parasite (2, 32).

The cytoplasmic structures of avian gametocytes have been fully described (1, 32). In addition to those organelles present in all blood stages of these parasites, mitochondria, ribosomes, and endoplasmic reticulum (ER) and pellicular cytostomes, the cytoplasm of mature gametocytes contains numerous "osmiophilic bodies" which are unit membrane bound, highly electron dense spherical structures with ducts connecting to the parasite plasmalemma. These organelles are believed to be involved in disrupting the host cell membranes during gametogenesis. The gametocyte of *P. gallinaceum* contains a Golgi apparatus (32) and a structure known as a "spherical body" (Fig. 3), which is also found in merozoites and young trophozoites of *P. gallinaceum* (1). The function of this organelle is unknown. It is similar in form to the male gamete nucleus as found in the zygote following fertilization (Fig. 9) and may thus be a source of confusion in interpreting the behavior of the male nucleus in the zygote. The cytoplasm of both male and female gametocytes of *P. gallinaceum* and other avian haemospornia contains a centriole consisting of a single central microtubule connected by filamentous spokes to a circle of nine individual microtubules, the entire structure being embedded in a matrix of electron-dense material (13, 16, 31, 32). The cytoplasm of the host cells of *P. gallinaceum*, whether containing gametocytes or asexual parasites, frequently contained electron lucent channels often associated with the host cell nucleus (Fig. 2).

The nucleus of the gametocytes of both sexes is surrounded by an envelope consisting of two membranes (Fig. 4, 7). The ground substance of the nucleus is of an uneven granular nature and contains, in the female only, a nucleolus (32). Neither spindle microtubules nor other indications of nuclear division are seen at this stage in the gametocyte nucleus.

Gametogenesis

Following a stimulus to undergo gametogenesis, changes in the gametocytes become apparent within one or two minutes (26). Two distinct sets of processes take place simultaneously: 1. The process of emergence whereby the gametocytes shed the enclosing host cell and 2. the intracellular changes within the gametocyte leading to the formation of gametes, most notably in the male gametocyte. Although these processes overlap in time to a considerable extent, they will be described separately.

i. Emergence of gametocytes from host cell

Within one or two minutes of being stimulated to undergo gametogenesis, both the gametocyte and the host cell loose their oval shape in the process of "rounding up". The subpellicular microtubules, reported to be occasionally present in the gametocytes of *P. gallinaceum* (2), were not seen in the rounded-up stages.

Accompanying the process of "rounding up", the disruption of the host cell membranes begins. In order to release a fully extracellular gametocyte, both the plasmalemma of the host RBC and the PVM must break down. These and other processes associated with emergence showed characteristic differences between male and female gametocytes.

In the male gametocyte, the PVM was invariably the first of the two host cell membranes to disintegrate. Fragments of the membrane collected in multilaminated myelin-like structures as plates or whorls in the cytoplasm of the host cell (Figs. 5, 6). At the same time, the cytoplasm of the host cell became filled with numerous unit membrane-bound, bleb-like vacuoles (Figs. 4-6) and the host cell cytoplasm rapidly lost electron density (Figs. 5, 6). The plasmalemma of the host RBC nevertheless remained morphologically intact as its soluble contents were apparently lost. The host cell nucleus, as well as the

fully rounded gametocyte and the multilaminate fragments of PVM, became tightly enclosed within the host cell plasmalemma (Fig. 5). Finally, the RBC plasmalemma may disintegrate, leaving a fully extracellular male gametocyte in the process of gametogenesis. Many male gametocytes, however, failed to disrupt the RBC plasmalemma before the release of the male gametes during exflagellation. In such cases, the male gametes became trapped within the host cell membrane.

Emergence of female gametocytes was a much more reliable process than that of male gametocytes. All surrounding host cell membranes were almost invariably shed by any female gametocyte of sufficient maturity to begin the process. The early stages of emergence of female gametocytes was similar to that of the males as the PVM broke down and collected in the host cell cytoplasm (Fig. 7). Only small collections of multilaminate membrane structures were found, however, never the whorls or plates seen with emerging male gametocytes. Nor were the bleb-like vacuoles in the host cell cytoplasm of emerging males seen with female gametocytes. However, in contrast to the male gametocyte, the plasmalemma of an RBC infected with a female gametocyte often disintegrated completely with total loss of host cytoplasmic contents before any signs of disruption appeared in the PVM. The PVM was subsequently shed and the female gametocytes almost invariably emerged as completely extracellular within 4 to 8 minutes of stimulation (Fig. 8).

Following the emergence of the gametocytes, the fate of the double membrane, lying beneath the gametocyte plasmalemma, was characteristically different according to sex. In the female gametocytes, this membrane, although discontinuous, remained intact following emergence and subsequent development (Fig. 8). In the male, however, the double membrane broke down at an early stage in male gametogenesis (Fig. 5 inset).

ii. Formation of the male gametes

Extensive activity in the nucleus and the cytoplasm began almost immediately after activation in the male gametocyte (Fig. 4). Cytoplasmic axonemes and intranuclear spindle microtubules appeared simultaneously as the nucleus underwent extensive lobe formation (Figs. 4, 6). The intranuclear spindle derived from an electron-dense pore in the nuclear membrane closely adjacent to a centriole-like structure in the cytoplasm, the "atypical centriole" described in gametocytes (Fig. 4). A lobe of the gametocyte nucleus passed into the exiting gamete closely opposed to the axoneme. As the nuclear lobes extended into the gametes, they acquired increasing electron density. These events were essentially similar to those described in other Haemosporina (13, 29, 30).

The extracellular male gametes were surrounded by a single unit membrane and contained a highly electron-dense nucleus surrounded by two-unit membranes. Occasionally, more than one nuclear body appeared to be present within a single male gamete. Usually one, but not infrequently two or even more axonemes were present in a single male gamete. The cytoplasm of the male gamete was otherwise totally devoid of contents other than a fine granular matrix. Ribosomes were notably absent. The male gamete was covered by a fine granular surface coat. Micrographs of male gametes were not shown, since many authors demonstrated them in the past (5, 7, 28, 29).

iii. The female gamete (Fig. 8)

On completing emergence, the female gametocyte is, in effect, a female gamete. As described above, the double membrane beneath the parasite's plasmalemma remains generally intact but is now interrupted at intervals by short gaps. The cytoplasm of female gametes contained essentially the same structures as were present in the intracellular gametocyte,

namely mitochondria, food vacuoles, endoplasmic reticulum, a Golgi complex, and numerous ribosomes and osmiophilic bodies, the latter now reduced in numbers. The nucleus remained generally compact, although lobe-like extensions were sometimes found. The nucleolus was generally contained in a pocket of the nuclear envelope. The four to six nuclear pores plugged with electron-dense material seen in the intracellular female gametocyte were associated in a regular arrangement with an equal number of electron-dense structures in the nucleoplasm (Fig. 8 inset). Nuclear microtubules were not seen within the nucleus of the female gamete.

Neither axonemes nor other cytoplasmic microtubules were present in unfertilized famale gametes. The surface of the female gamete was covered by a fine granular coat.

Fertilization

Fusion of the plasmalemmas of male and female gametes has previously been described during fertilization in malaria parasites (16, 30). Our observations were consistent with this interpretation. Although subsequent fusion with additional male gametes is apparently prevented, as observed by light microscopy, no obvious immediate changes were noted in the membrane of the fertilized female gamete, which might account for its refractoriness to multiple fertilizations.

Shortly after gamete fusion, a process largely effected within 15 to 20 minutes of initiation of gametogenesis (9), a number of changes were observed in the female gamete or zygote, as it may now be called. A large gap in the double inner membrane of the cell appeared reflecting increased surface area presumably due, at least in part, to fusion of the cell membranes of male and female gametes.

The axoneme and nucleus of the male gamete remained in recognizable form in the cytoplasm of the zygote at this time (Fig. 9). The male

nucleus remained electron-dense although less so than in the male gamete. It was enclosed by an envelope of two-unit membranes, as in the gamete, but was now closely surrounded by a third membrane (Fig. 9) which appeared to be an extension of the endoplasmic reticulum (ER) of the female gamete. The male nucleus appeared to travel through a channel of ER to a region of the female nucleus in which the nuclear envelope was thrown into a complex of convoluted folds (Fig. 10). The outer membrane surrounding the male nucleus (i.e., that presumed to be continuous with the ER) became continuous with the outer membrane of the nuclear envelope (NE) closely adjacent to the convoluted region. At this point, therefore, male and female nuclei were surrounded by the same membrane continuous with the outer envelope of the NE of the female nucleus.

Transformations in the zygote

While these events were in progress, the nucleus and cytoplasm of the fertilized female gamete underwent other changes. The nucleus and the cell itself become polarized. The nucleus of the zygote elongated in the form of a cone, whose apex extended towards the cell membrane distal to the nucleolus, which invariably lay in a pocket at one side of the base of the cone (Fig. 11). The tip of the cone was closely associated with two cytoplasmic centrioles (Fig. 12) from which region bundles of cytoplasmic microtubules radiated around the nucleus towards its' base (Figs. 12, 13, 14). At the apex of the nucleus, electron dense material was deposited just below the plasmalemma of the parasite (Fig. 14). These events occurred within 2 hours after gamete fusion.

The electron dense material deposited at the nuclear apex is the anlage of the incipient apical complex and the triple membraned pellicular complex, which will eventually surround the mature ookinete (Fig. 15).

Beneath the zygote plasmalemma, an inner membrane appeared and beneath this, the electron dense material deposited at the apex of the nucleus gave rise to a third dense membrane (Fig. 15, inset). By 8 to 10 hours post fertilization, the formation of the apical complex had progressed to the point where subpellicular microtubules began to extend beneath the pellicle, and the deposit of electron dense material, the developing canopy, extended away from the apex (Fig. 16). At the apex itself, the "polar rings" became visible as distinct structures, and the whole complex began to protrude from the side of the previously spherical zygote. The nucleus was, by this time, no longer extended in a cone toward the site of the apical complex formation and had retracted to the center of the cell.

At about the same time (8 to 10 hours), as these developments were occurring, other changes were taking place in the cytoplasm. Extensive endoplasmic reticulum (ER) appeared and the crystalloid began to be laid down by an expansion of the ER. In the region of the apical complex, the electron dense bodies, similar in appearance to the osmiophilic bodies of gametocytes, appeared as the precursors of the micronemes of the mature ookinete (Fig. 17).

From about this point in time onward, therefore, all the structures and organelles of the mature ookinete were present at least in incipient form. Elongation of the ookinete continued to completion by 18 to 24 hours post fertilization and was characterized largely by an extension of the pellicular complex and a proliferation of micronemes. The nucleolus was retained throughout the developmental process and, as the ookinete approached maturity, the nucleus acquired a compact oval shape with patches of heterochromatin in the nucleoplasm (Fig. 17). Although occasionally seen in early zygotes, intranuclear spindles were not seen

during subsequent maturation of the ookinetes. The structures in the anterior 1/3 of a mature ookinete are illustrated in cross-sections in Figs. 18-21.

Unfertilized female gamete (Fig. 22).

Female gametes, which had been prevented from being fertilized, underwent none of the changes described above for zygotes after incubation for 24 hours under identical culture conditions. The cell and cytoplasm, although structurally intact and viable up to this point, were devoid of most structures and organelles with the exception of hemozoin containing food vacuoles, mitochondria, and the still numerous ribosomes. The cell was mainly surrounded by a single unit membrane. Interestingly, however, there were at various points beneath the cell membrane deposits of electron dense material (Fig. 22, inset) reminiscent of those deposited in the zygote in the early stages of ookinete formation.

DISCUSSION

The observations made in this study cover the events involved in the transformation of male and female gametocytes of *P. gallinaceum*, as found in the circulation in the avian host, through to the formation of the mature ookinete, the final stage of development of the parasite in the midgut of the mosquito vector. Although these transformations have been subject to several studies in various species of malaria parasites and other Haemosporina, certain aspects analyzed in some detail in the present study have not been adequately described previously for malaria parasites. These areas are i) the nature of the parasitophorous vacuole of gametocytes and the processes of emergence of male and female gametocytes from their host cells, ii) the behavior of male and female gamete nuclei immediately after fertilization, and iii) the early ultrastructural events in the transforming zygote.

The structures of the intracellular gametocytes of *P. gallinaceum* found in the present study conform to previous observations of gametocytes of avian plasmodia (2, 31) and are closely related to those of avian *Haemoproteidae* (5, 13). Although evident from published data (2), it has not previously been noted that the parasitophorous vacuole is of similar electron density to that of the host cytoplasm, in contrast to the electron lucent vacuole of asexual trophozoites. The significance of this observation is unclear except that it appears to be a universal characteristic in avian malarias, at least, and suggests the possibility of functional differences between the PVM/s of gametocytes and asexual parasites.

Following activation by a suitable stimulus, gametocytes (25, 26) undergo a series of rapid transformations, leading to formation of male or female gametes and fertilization. The nuclear events involved and the actual formation of the gametes have been well described by previous investigators (5, 7, 13, 16, 28-31); the observations recorded here for *P. gallinaceum* are generally consistent with them. The process by which the activated gametocytes of *Plasmodium* emerge from their host cells has not previously been fully described at an ultrastructural level. We have demonstrated here that the male and female gametocytes have characteristic differences in mediating this process. The main difference between them lies in the relative efficiency with which the plasmalemma of the host cell is disrupted. In the case of the female, this is mediated very effectively and frequently precedes disruption of the PVM. In contrast to the plasmalemma of the host cell, the PVM is disrupted with similar effectiveness by gametocytes of either sex. As a consequence of this difference in male and female gametocyte emergence, the mature female gametes are almost invariably found to be devoid of adhering host cell membranes.

Male gametocytes, on the other hand, are frequently found to be enclosed in the host cell membrane during male gamete formation (exflagellation), together with the nucleus of the avian red blood cell. Similar observations by light microscopy by Dresser et al. (15) on *Leucocytozoon simondi* suggest that this difference in behavior of male and female gametocyte may be a general characteristic of the *Haemosporina*.

Based on our present observation, together with others made by previous investigators, we are able to define the characteristic features which allow distinction between male and female gametocytes following activation. This is an important and otherwise not always obvious distinction which allows us to determine whether, for instance, a cell containing an axoneme is an exflagellating male gametocyte or a fertilized female gamete. The main distinctions, previously noted between male and female gametocytes, have been the relatively high density of cytoplasmic ribosomes and relatively compact nucleus in the female, compared to the male gametocyte (1). While this distinction is broadly true, it is frequently hard to distinguish the sexes on these criteria. In avian malaria parasites, the most unequivocal distinction, if visible in an E.M., section, is the presence of a nucleolus in the female; an organelle never seen in the male gametocyte. Following activation, extensive lobe formation of the nucleus and the appearance of many axonemes can readily identify a male gametocyte. However, as pointed out, axonemes and also nuclear lobes may occur in cross-sections of fertilized female gametes. Cytoplasmic centrioles, associated with the nuclear envelope, are also present in gametocytes of both sexes. The pattern of disruption of host cell and PV membranes may, as described above, provide a good indication of the sex of an activated gametocyte, while the actual formation of the male gametes themselves obviously defines the sex of the gametocyte. However, none of these indicators of sex may be evident in an E.M. section.

One property of gametocytes of avian malarias becomes evident shortly after activation which has been, in our experience, a completely reliable indicator of sex and is evident in almost any section. This is the previously unnoted property whereby the double membrane of the male gametocyte becomes disrupted into numerous short fragments, shortly after activation. In contrast, the corresponding double membrane of the female remains extensively continuous over large areas and even when significant discontinuities appear in it following fertilization, these occur in one or two large areas, leaving the double membrane mainly continuous elsewhere.

By applying these, and especially the latter criterion for sex determination, we have been able to confidently follow the fate of the male gamete, its' axoneme and nucleus during fertilization of female gametes. Fusion of the cell membranes of male and female gametes of *Haemosporina* during fertilization has been previously reported by several workers (16, 30). Following gamete fusion, subsequent entry of other male gametes is apparently prevented according to observations by light microscopy, in which many additional male gametes usually attach to but do not enter a fertilized female (26),. No changes were recognized at an ultrastructural level in the female gamete, which indicates a mechanism for preventing multiple fertilizations.

The only apparent alteration in the membranes of the female gamete noted here, in association with the time of fertilization, was the appearance of a large gap in the double inner membrane. This gap reflects an increase in the surface area of the outer membrane or plasmalemma of the female gamete and is presumably due, at least in part, to fusion of the cell membranes of male and female gametes. It may be estimated from the dimensions of male and female gametes that between 1/6 and 1/5 of the surface membrane of the zygote is contributed by the male gamete (see Appendix). Expansion of the

plasmalemma of the female gamete may also precede fertilization, as has been reported for *P. falciparum* (29). Following fusion of male and female gametes, the axoneme of the male now lies free in the cytoplasm of the female, as has been observed in several previous studies (13, 16, 30). The male gamete nucleus, on the other hand, was seen in our studies to be enclosed in a channel of endoplasmic reticulum, a phenomenon not previously recorded. This association of the male nucleus with the female ER appeared to be maintained up to the point of fusion of male and female nuclei in a region adjacent to a complex of convolutions in the envelope of the female nucleus.

Almost immediately following fusion of male and female gametes and probably even before fusion of their nuclei the nucleus of the female gamete begins to polarize in a process similar to that described in *Haemoproteus* (17) but not previously in *Plasmodium*. The nucleus extends at a point distal to the nucleolus. The convoluted nuclear membranes are seen in close association with the zygote membrane showing a gap in the double inner membrane. This extension of the nucleus, in association with two cytoplasmic centrioles, is the prelude to the deposition of the structures of the apical complex and appears to be a general phenomenon in this group of parasites at this stage of their development. However, whereas in our observations on *P. gallinaceum*, the extension of the nucleus was associated with the presence of two bundles of microtubules in the cytoplasm and the absence of microtubules in the nucleus in the study *H. columbae* (17), the reverse was true. As pointed out by Gallucci (17), the involvement of centrioles or indeed the nuclear extension reported here, in association with the formation of the apical complex, has not been reported in any other life cycle stage of this group of parasites.

By about 8 to 12 hours post fertilization, all the essential structures and organelles of the mature ookinete appear to be present as previously

described (24). The subsequent development of the zygote, as it matures into an ookinete, consists essentially of an elongation of the apical end leading to the transformation from a spherical zygote to the elongated form of the mature ookinete, whose structures have been described in previous studies on related *Haemosporina* (8, 12, 14, 17-20, 33).

We have also observed the behavior of unfertilized female gametes of *P. gallinaceum* maintained under the same *in vitro* conditions as those which supported the transformation of fertilized zygotes into mature and functional ookinetes. Such unfertilized female gametes remained almost entirely devoid of new structures. It was interesting to note, however, that deposits of electron dense material were found beneath the plasmalemma of such parasites, similar to those deposited in the early stages of the transformation of the fertilized zygotes. It appears, therefore, that while the stimulus of fertilization is necessary for the full process of ookinete formation, limited development takes place in the female gamete even without this event. Similar limited synthesis of surface proteins, otherwise associated with the ookinete stage, has also been found to take place in such unfertilized female gametes (Carter and Kaushal, unpublished observations).

APPENDIX

The approximate surface areas of male and female gametes may be estimated from their dimensions. The female gamete of P. gallinaceum is a sphere with a diameter of about 6μ. The dimensions of a male gamete of P. gallinaceum are essentially those of a cylinder about 20μ in length and 0.4μ in diameter.

The surface area of the female gamete is thus derived from the formula for the surface area of a sphere, $4\pi r^2 = 4 \times 3.14 \times 3^2 \times \mu^2 \cong 110\mu^2$.

The surface area of the male gamete is derived from the formula for the surface area of a cylinder, $2\pi r \times \text{length} + 2\pi r^2 = 2\pi r\ (\text{length} + r) \cong 2 \times 3.14 \times 0.4 \times 20\mu^2 \cong 24\mu^2$.

The total surface area of the zygote is thus 130 to $140\mu^2$ of which between 1/6 and 1/5 is contributed by the male gamete.

REFERENCES

1. Aikawa, M. 1966. The fine structure of the erythrocytic stages of three avian malarial parasites, Plasmodium fallax, P. lophurae and P. cathemerium. Am. J. Trop. Med. Hyg., 15:449-471.
2. Aikawa, M., Huff, C. G. and Sprinz, H. 1969. Comparative fine structure study of gametocytes of avian, reptilian and mammalian malarial parasites. J. Ultrastruc. Res. 26:316-331.
3. Aikawa, M., Huff, C. G. and Strome, C. 1970. Morphological study of microgametogenesis of Leucocytozoon simondi. J. Ultrastruct. Res. 32:43-68.
4. Aikawa, M., Rener, J., Carter, R. and Miller, L. H. 1981. An electron microscopical study of the interaction of monoclonal antibodies with gametes of the malarial parasite Plasmodium gallinaceum. J. Protozool. 28:383-388.
5. Aikawa, M. and Sterling, C. R. 1974. Intracellular parasitic protozoa. Academic Press, New York.
6. Bradbury, P. C. and Roberts, J. F. 1970. Early stages in differentiation of gametocytes of Haemoproteus columbae Kruse. J. Protozool. 17:405-414.
7. Bradbury, P. C. and Trager, W. 1968. The fine structure of microgametogenesis in Haemoproteus columbae Kruse. J. Protozool. 15:700-712.
8. Canning, E. U. and Sinden, R. E. 1973. The organization of the ookinete and observatoins on nuclear division in oocysts of Plasmodium berghei. Parasitology 67:29-40.

9. Carter, R., Gwadz, R. W. and Green, I. 1979. Plasmodium gallinaceum: Transmission blocking immunity in chickens. II. The effect of antigamete antibodies in vitro and in vivo and their elaboration during infection. Expl. Parasitol. 47:194-208.

10. Chen, D. H., Seeley, D., and Good, C. 1977. In vitro P. berghei ookinete formation. V. Internat. Congr. Protozool. N. Y. Abstr. no. 21.

11. Davies, E. E. 1974. Ultrastructural studies on the early ookinete stage of Plasmodium berghei nigeriensis and its transformation into an oocyst. Ann Trop. Med. Parasitol. 68:283-290.

12. Desser, S. S. 1970. The fine structure of Leucocytozoon simondi. III. The ookinete and mature sporozoite. Can. J. Zool. 48:641-645.

13. Desser, S. S. 1972. Gametocyte maturation, exflagellation and fertilization in Parahaemoproteus (= Haemoproteus) velans (Coatney and Roudabush) (Haemosporina: Haemoproteidae): An ultrastructural study. J. Protozool. 19:287-296.

14. Desser, S. S. 1972. The fine structure of the ookinete of Parahamoproteus velans (= Haemoproteus) velans. (Coatney and Roudabush) (Haemosporidia: Haemoproteidae). Can. J. Zool. 50:477-480.

15. Desser, S. S., Fallis, A. M., and Allison, F. R. 1976. Nuclear changes preceeding microgamete formation in Leucocytozoon simondi and Leucocytozoon tawaki. Can. J. Zool. 54:799-801.

16. Gallucci, B. B. 1974. Fine structure of Haemoproteus columbae Kruse during macrogametogenesis and fertilization. J. Protozool. 21:254-263.

17. Gallucci, B. B. 1974. Fine structure of Haemoproteus columbae Kruse during differentiation of the ookinete. J. Protozool. 21:264-275.

18. Garnham, P. C. C., Bird, R. G. and Baker, J. R. 1962. Electron microscope studies of motile stages of malaria parasites. III. The ookinetes of Haemamoeba and Plasmodium. Trans. Roy. Soc. Trop. Med. Hyg. 56:116-120.

19. Garnham, P. C. C., Brid, R. G., Baker, J. R., Desser, S. S. and El-Nahal, H. M. S. 1969. Electron microscope studies on motile stages of malaria parasites. IV. The ookinete of Plasmodium berghei yoelii and its transformation into the early oocyst. Trans. Roy. Soc. Trop. Med. Hyg. 63:187-194.

20. Gass, R. F. 1979. The ultrastructure of cultured Plasmodium gallinaceum ookinetes: A comparison of intact stages with forms damaged by extracts from blood fed, susceptible Aedes aegypti. Acta. Tropica. 36:323-334.

21. Gass, R. F. and Yeates, R. A. 1979. In vitro damage of cultured ookinetes of Plasmodium gallinaceum by digestive proteinases from susceptible Aedes aegypti. Acta Tropica. 36:243-252.

22. Howard, R. J., Kaushal, D. C. and Carter, R. 1982. Radioiodination of parasite antigens with 1,3,4,6, - tetrachloro-3α, 6α - diphenylglycouril (IODOGEN): Studies with zygotes of Plasmodium gallinaceum. J. Protozool. 29:114-117.

23. Kaushal, D. C., Carter, R., Howard, R. and McAuliffe, F. M. 1983. Characterization of antigens of mosquito midgut stages of Plasmodium gallinaceum. I. Zygote surface antigens. J. Mol. Biochem. Parasitol. 8:53-69.

24. Melhorn, H., Peters, W. and Haberkorn, A. 1980. The formation of kinetes and oocyst in Plasmodium gallinaceum (Haemosporidia) and considerations on phylogenetic relationships between Haemosporidia, piroplasmida and other coccidia. Histologica, 15:135-154.

25. Nijhout, M. M. 1979. Plasmodium gallinaceum: Exflagellation stimulated by a mosquito factor. Exp. Parasitol. 48:75-80.

26. Nijhout, M. M. and Carter, R. 1978. Gamete development in malaria parasites. Bicarbonate-dependent stimulation by pH in vitro. Parasitology 76:39-53.

27. Rener, J., Carter, R., Rosenberg, Y. and Miller, L. H. 1980. Anti-gamete monoclonal antibodies synergistically block transmission of malaria by preventing fertilization in the mosquito. Proc. Natl. Acad. Sci. USA 77:6797-6799.

28. Sinden, R. E. 1975. Microgametogenesis in Plasmodium yoelii nigeriensis: A scanning electron microscope investigation. Protistologica 11:263-268.

29. Sinden, R. E., Canning, E. U., Bray, R. S. and Smalley, M. E. 1978. Gametocyte and gamete development in Plasmodium falciparum. Proc. R. Soc. Lond. B. 201:375-399.

30. Sinden, R. E., Canning, E. U., and Spain, B. 1976. Gametogenesis and fertilization in Plasmodium yoelii nigerienssis: A

transmission electron microscope study. Proc. R. Soc. Lond. B. 193:55-76.

31. Sterling, C. R. 1972. Ultrastructural study of gametocytes and gametogenesis of Haemoproteus metchnikovi. J. Protozool. 19:69-76.

32. Sterling, C. R. and Aikawa, M. 1973. A comparative study of gametocyte ultrastructure in avian Haemosporidia. J. Protozool. 20:81-92.

33. Trefiak, W. D. and Desser, S. S. 1973. Crystalloid inclusions in species of Leucocytozoon, Parahaemoproteus and Plasmodium. J. Protozool. 20:73-80.

FIGURE LEGENDS

Note: All electron micrographs are of *P. gallinaceum*.

Fig. 1. Female gametocyte before activation within a red blood cell. The gametocyte is enclosed by the parasitophorous vacuole membrane (PVM). Beneath the PVM lies the plasmalemma of the parasite (single arrow) and beneath this, the double layered membrane (double arrow) characteristic of the gametocyte pellicle. In addition to mitochondria (M) and endoplasmic reticulum, osmiophilic bodies (Ob), characteristic organelles of gametocytes, are present in the cytoplasm of the parasite. X 27,000. Inset: High magnification micrograph showing the parasitophorous membrane and gametocyte membrane. X 30,000.

Fig. 2. Unit membrane bound blebs or vesicles (arrow) are seen in the erythrocyte infected with gametocytes. X 32,000.

Fig. 3. Electron micrograph showing a spherical body (Sb) and mitochondria (M) of gametocytes. X 27,000.

Fig. 4. Activated male gametocyte. Axonemes (A) are present in the cytoplasm. A centriole (C) is adjacent to electron-dense nuclear material (arrow) and intranuclear spindle (Ns). The nucleus (N) itself has become lobed. Membrane-bound blebs and vesicles are present in the erythrocyte cytoplasm (double arrow). The PVM is still largely intact. X 33,000.

Fig. 5. An activated male gametocyte in which the PVM has disrupted completely and collected as multilaminated membrane whorls (W) in the host cytoplasm. The hose cell membrane remains intact retaining the host cell nucleus (HCN). The host cytoplasm has lost electron density and is filled with numerous membrane-bound blebs (arrows). X 26,500. Inset: Activated male gametocyte in which the plasmalemma of the host cell (arrows) has not disrupted and now tightly encloses the parasite. The inner membrane of the gametocyte has begun to break down (double arrow). X 24,000.

Fig. 6. Intracellular activated male gametocyte. The condition of the cytoplasm, the PVM and host cell plasmalemma, the configuration of the parasite nucleus (N) and the dispersion of axonemes (A) all indicate that the gametocyte has reached a more advanced stage of gametogenesis than that in Fig. 5. Note many multilaminated membrane whorls (arrow) and vesicles (V) in the erythrocyte cytoplasm. X 25,000. Inset: Higher magnification micrograph of intranuclear spindles (arrow) in the nuclei. X 50,000.

Fig. 7. An activated female gametocyte in which the PVM has already disrupted and collected as multilaminated structures (single arrow) in the cytoplasm of the host cell. The host cell plasmalemma (double arrows) shows signs of disruption. The nucleus (N) of the gametocyte contains a nucleolus (Nc). X 30,000.

Fig. 8. An extracellular female gamete. The plasmalemma is covered with a fine fibrillar surface coat (arrow). The inner membrane of the gametocyte is indicated by a double arrow. A nucleus (N) with a nucleolus (Nc), mitochondria (M) and Golgi complex (G) are present. X 41,000. Inset: Nucleus (N) of an extracellular female gamete showing regular arrangement of nuclear pores (single arrow) and electron dense patches (double arrow) within the nucleoplasm. X 30,000.

Fig. 9. Zygote containing an axoneme (A) and a male gamete nucleus (Mn). The male nucleus is enclosed in endoplasmic reticulum (ER). A tangential section of the nuclear membrane of the female gamete shows a series of pores (arrow). X 49,000.

Fig. 10. A zygote showing convoluted folds (arrow) of the nuclear membrane. A male nucleus (Mn) is present adjacent to the folds. X 25,000.

Fig. 11. A zygote showing the polarization of the nucleus (N) as the zygote begins to differentiate to become an ookinete. Note the nucleus is triangular in shape. A cone (arrow) is formed distal to the nucleolus (Nc) and is closely associated with the zygote cell membrane. X 21,000.

Fig. 12. High magnification electron micrograph of a zygote. The tip of the nuclear cone (arrow) is closely associated with two centrioles (C), from which region bundles of microtubules (Mt) radiate around the nucleus (N) towards its base. Electron dense material (D) is also present between the tip of the nuclear cone and the plasma membrane. X 42,000.

Fig. 13. A zygote showing bundles of microtubules (Mt) radiating around the nucleus (N) from the electron dense zone (D). X 33,000.

Fig. 14. Apical region of the zygote nucleus showing an appendix-like extension (NAP) of the nucleus extending in the direction of the apex. Microtubules (Mt) which originate from the electron dense material (D), radiate through the cytoplasm on either side of the nucleus. X 32,000.

Fig. 15. As transformation of the zygote to an ookinete progresses, the triple membrane pellicular complex (arrow) which will eventually surround the mature ookinete becomes evident. Subpellicular microtubules (Mt) appear just beneath the pellicular complex and the crystalloid (Cr) begins to be laid down within expanded endoplasmic reticulum. X 33,000. Inset: High magnification micrograph showing triple pellicular membranes. A fine line (arrow) between the 2nd and 3rd membrane can be seen. X 38,000.

Fig. 16. A longitudinal section of the apical end of a mature ookinete. Polar rings (Po), a canopy (Ca), subpellicular cavity (Sc), subpellicular microtubules (Mt) and micronemes (Mi) are present. X 40,000.

Fig. 17. Electron micrograph of mature ookinetes. The apical end contain many micronemes (Mi), a nucleus (N) is situated in the midportion and the main body of the crystalloid (Cr) is in the posterior end. X 8,300.

Fig. 18. An ookinete cross-sectioned at the level of the apical end. Relationship between triple membraned pellicle, an electron dense canopy (Ca), a subpellicular cavity (Sc), subpellicular microtubules (Mt) and micronemes (Mi) is clearly demonstrated. X 50,000.

Fig. 19. A cross section of the ookinete cut at a level just posterior that in Figure 18. The subpellicular cavity (Sc) begins to form subcompartments. Also, ribs (arrow) extend inward from the canopy (Ca). X 50,000.

Fig. 20. A cross section of the ookinete cut at a level posterior to that in Figure 19. Subcompartments of the subpellicular cavity (Sc) and canopy's ribs (arrow) become more evident. A microtubule (Mi) runs along side each rib. X 50,000.

Fig. 21. A cross section of the ookinete at the midportion. The nucleus (N) and subpellicular microtubules (Mt) can be seen. The canopy is no longer present and the three membraned structure of the ookinete pellicle is evident. X 50,000.

Fig. 22. Electron micrograph of unfertilized female gamete after 24 hours in culture. The cell is mainly surrounded by a single membrane. However, there are at various points deposits of electron dense material beneath the cell membrane (arrow). X 27,000. Inset: High magnification micrograph showing electron dense material along the cell membrane. X 60,000.

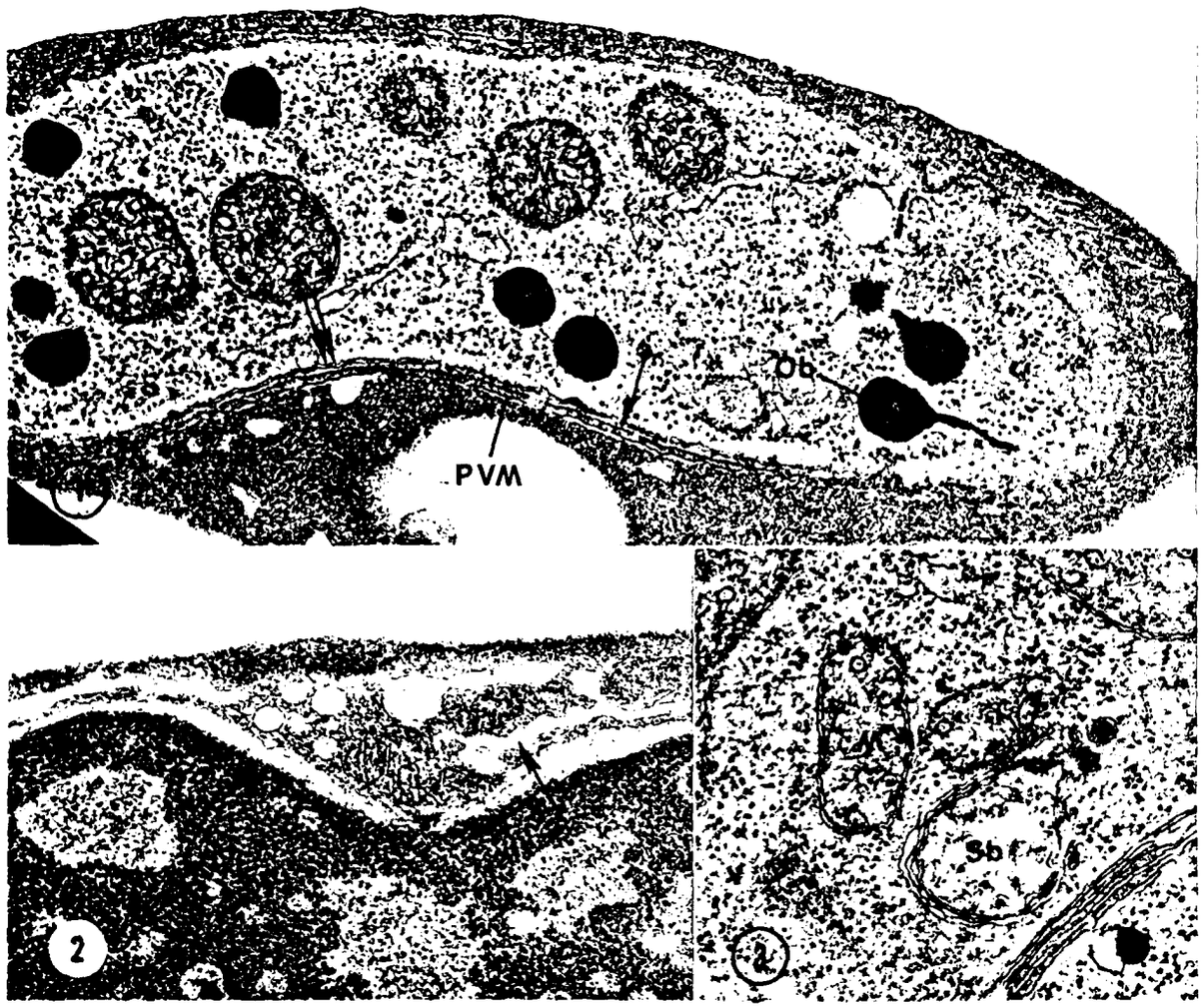
Ob
PVM
1
2
Sb
2

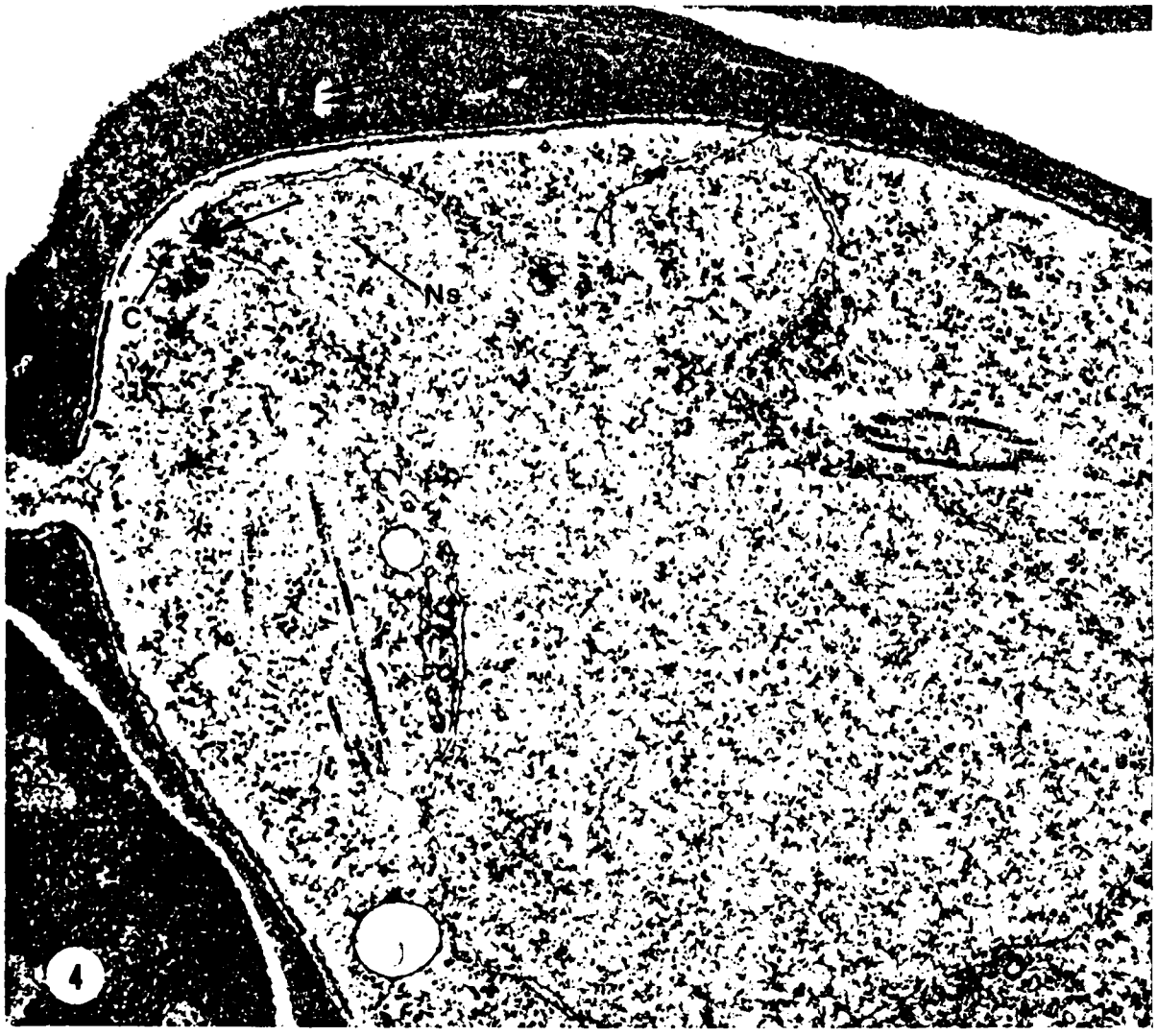
C
Ns
A
4

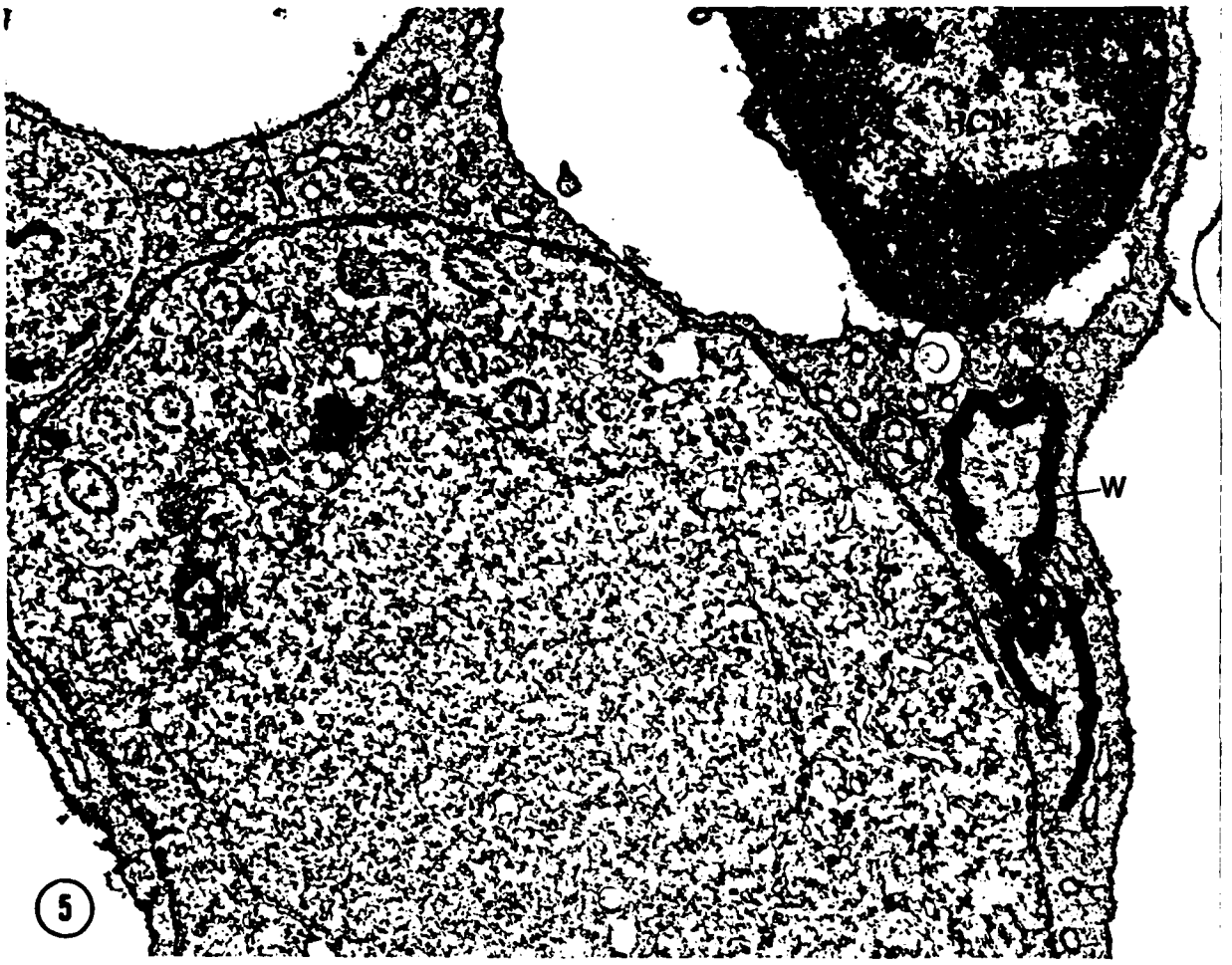
W
5

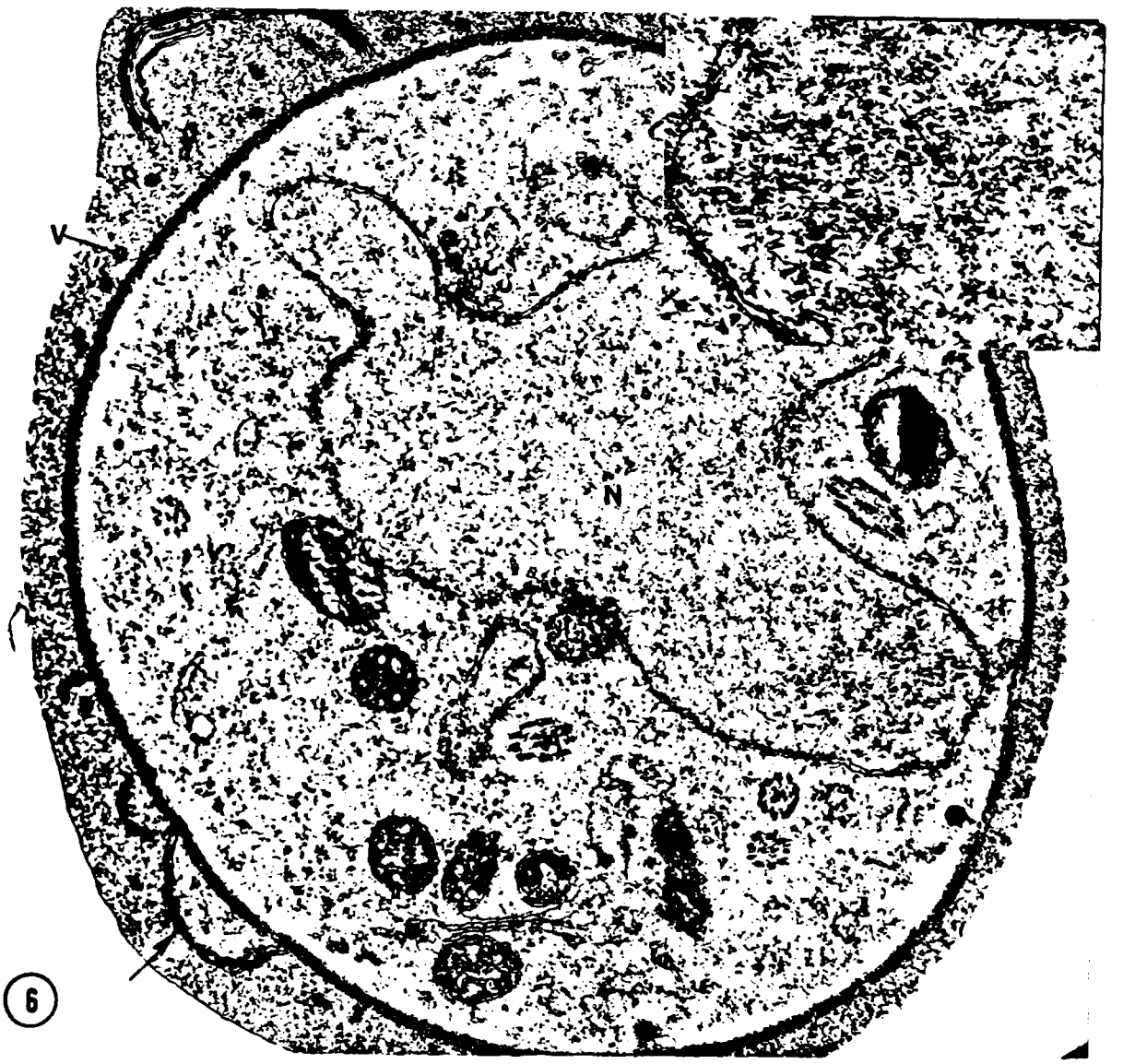

6

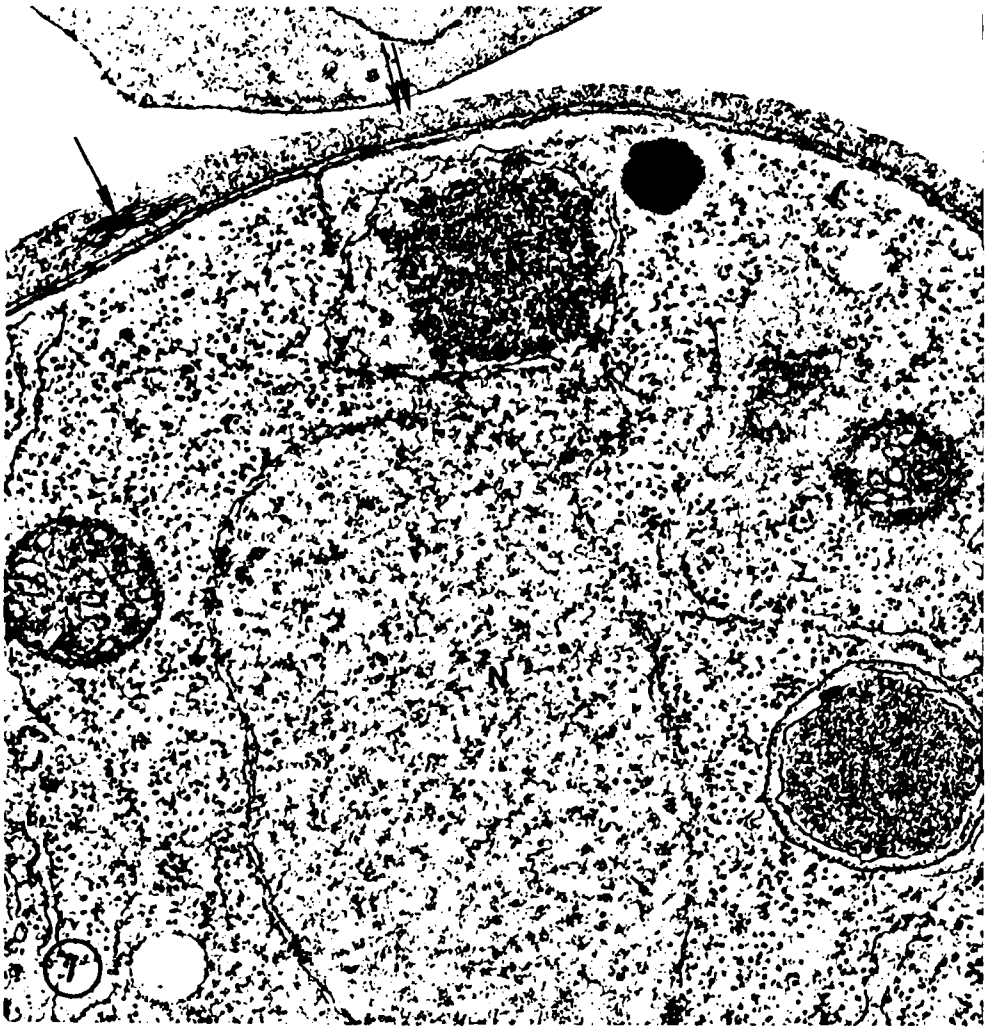
N

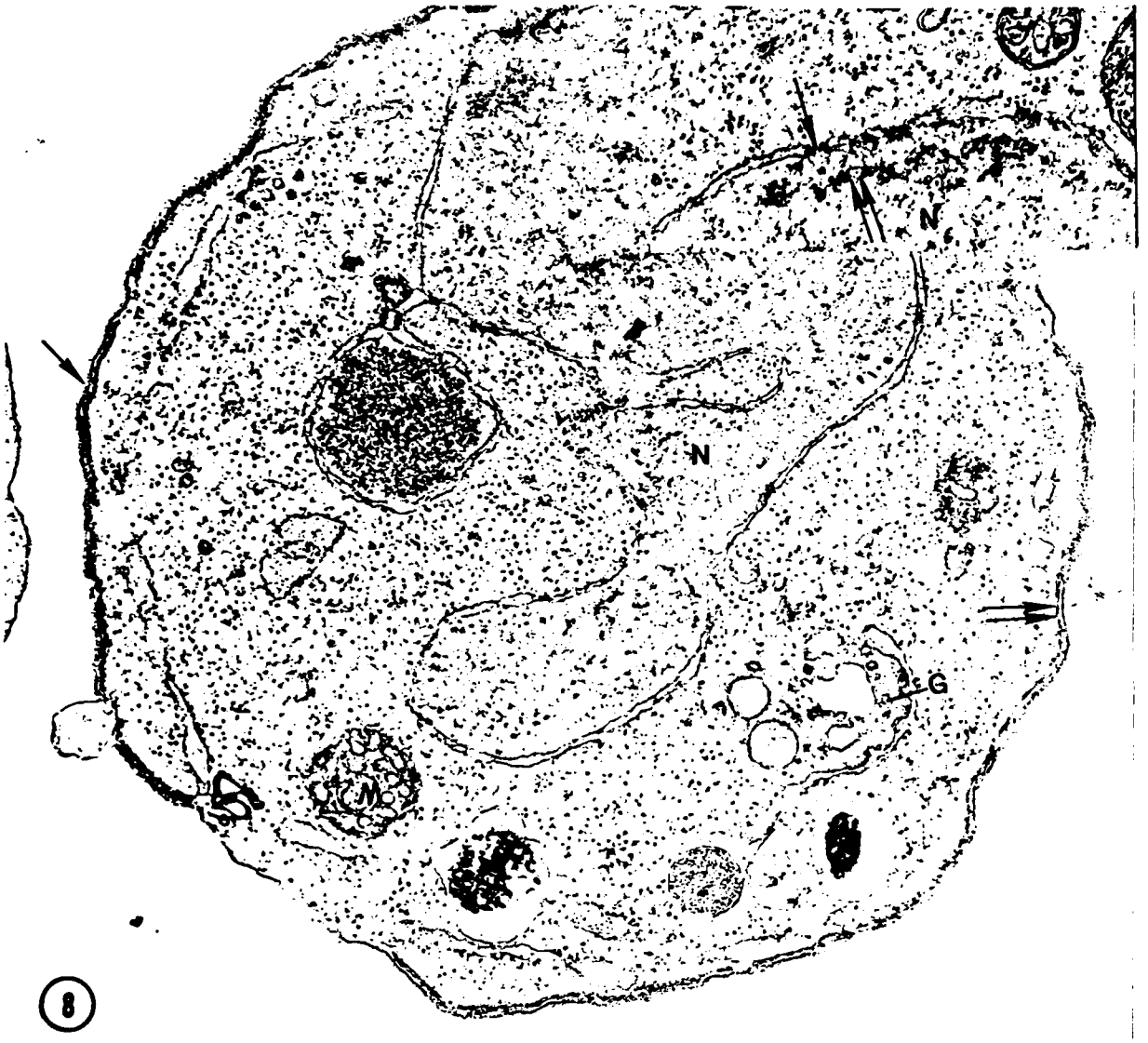

(8)


A
ER
Mp
Mn
10

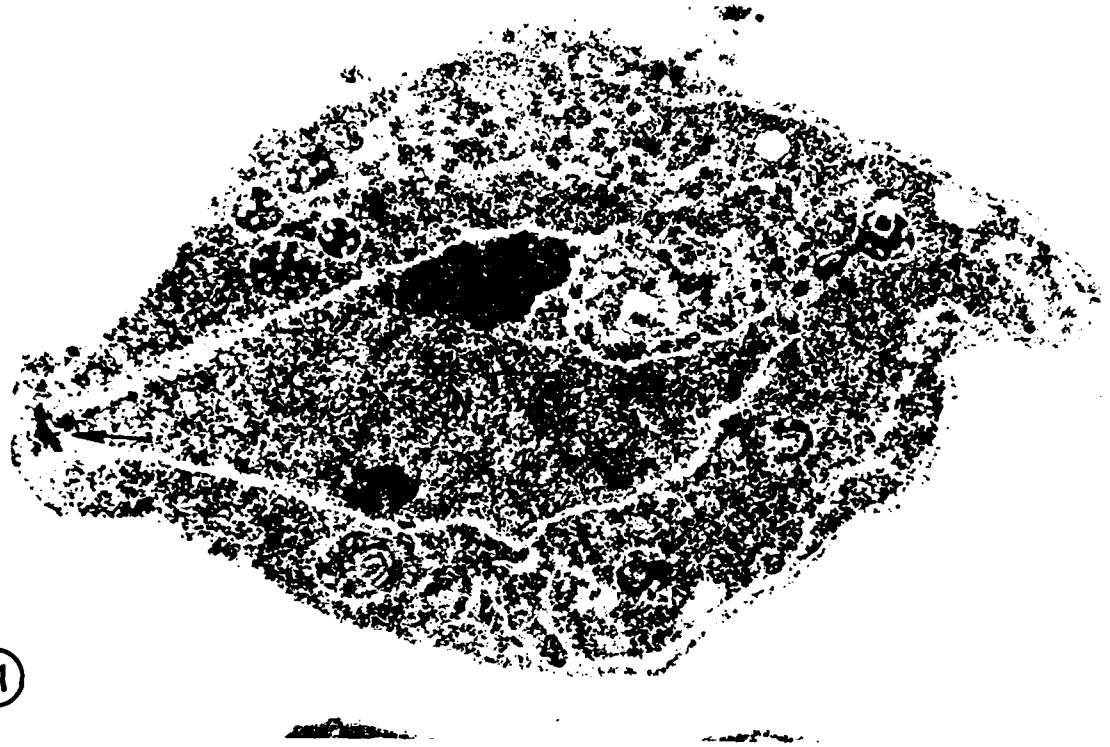

(11)


C
Mt
N
12
Mt
N
13

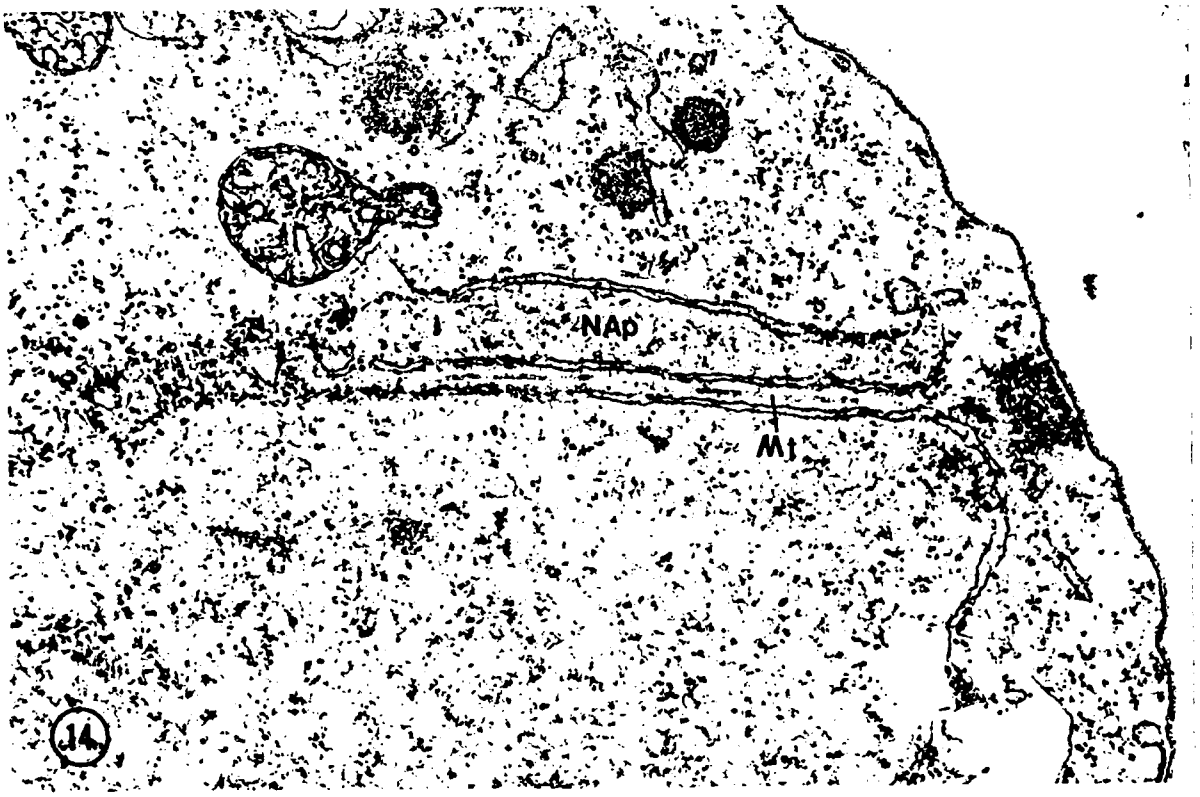
NAp
M1
14

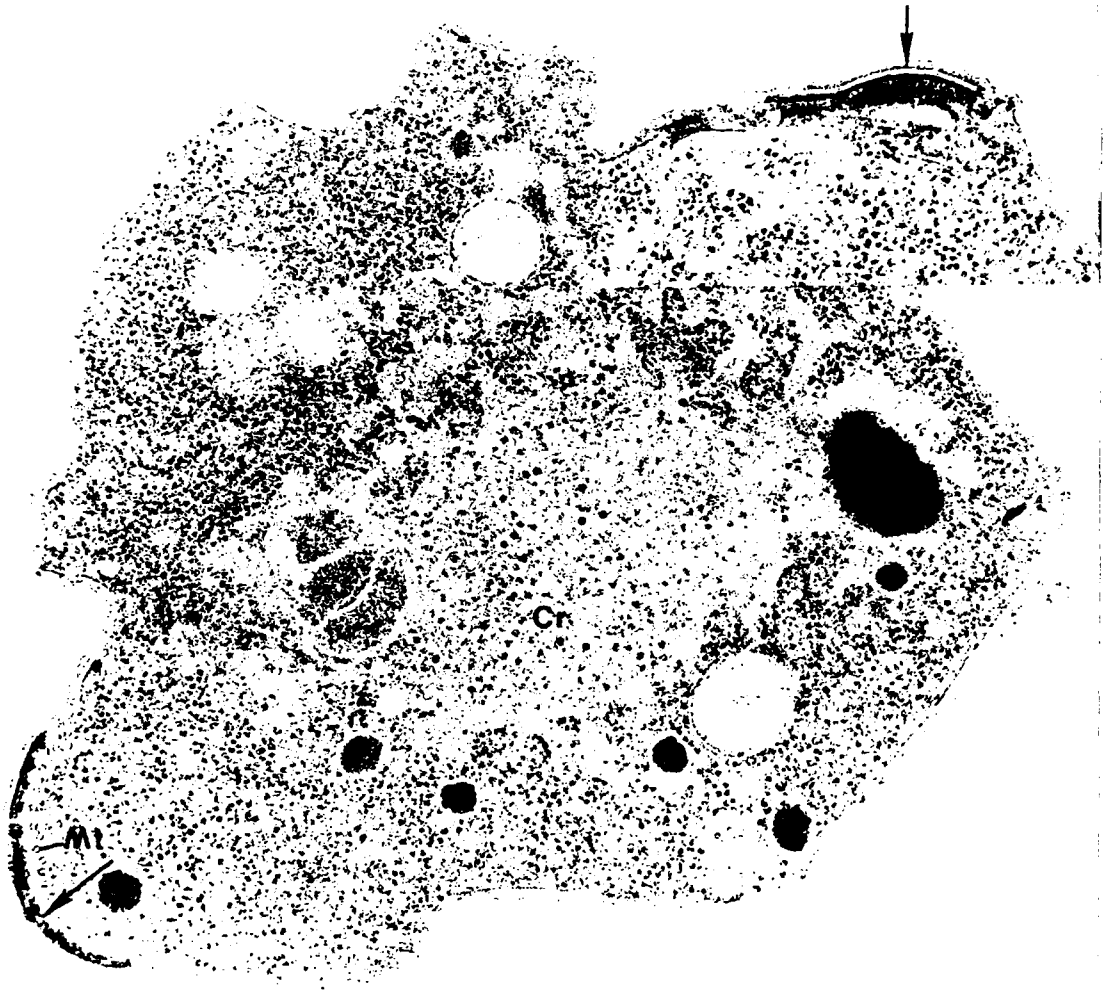

(15)

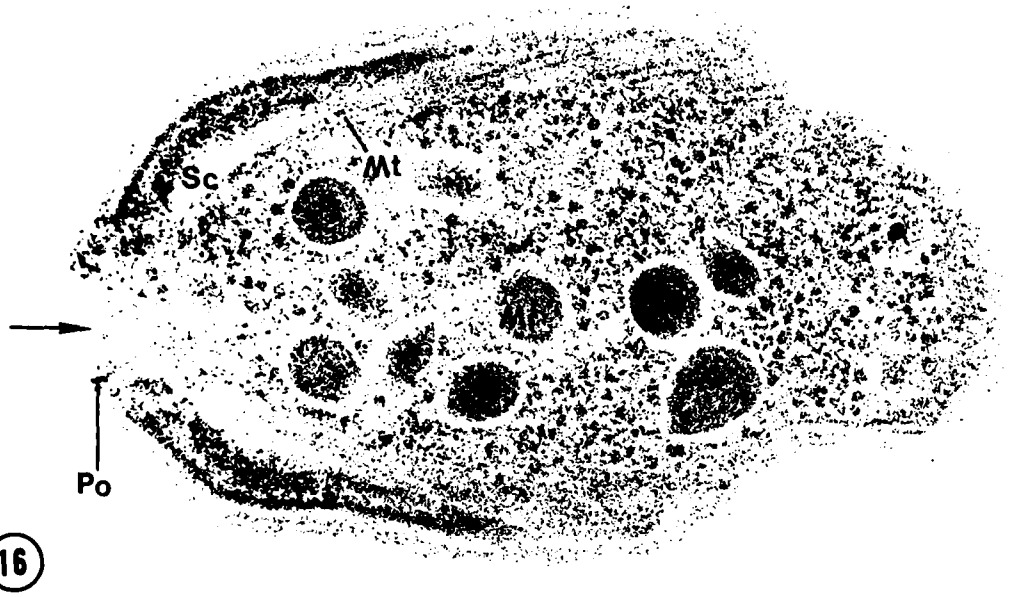

(16)

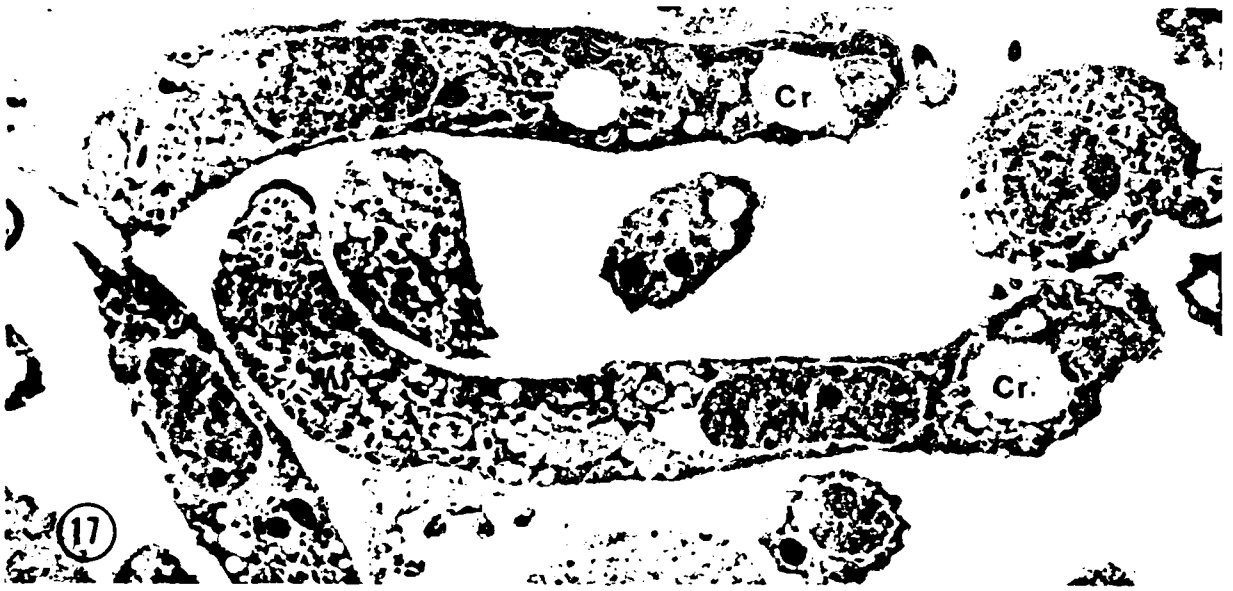
Cr.
Cr.
17

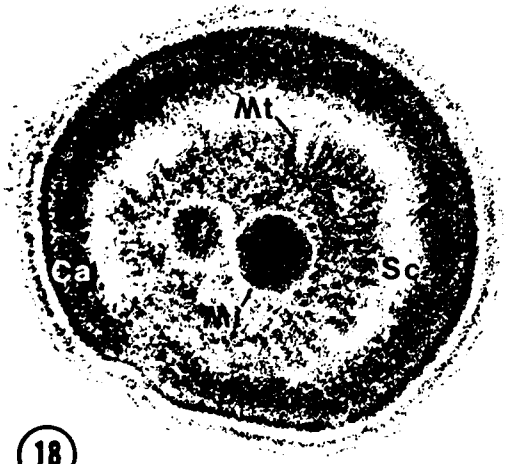

18

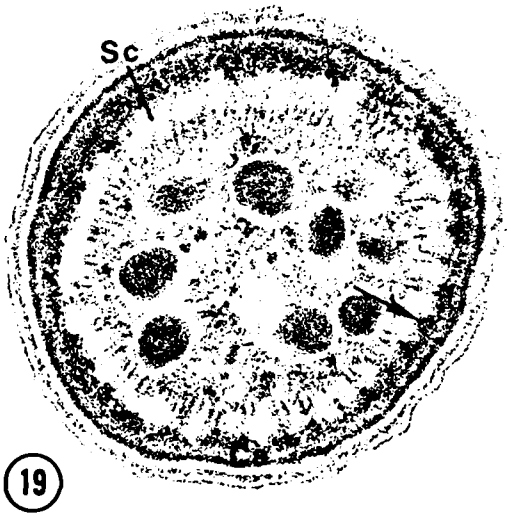

19

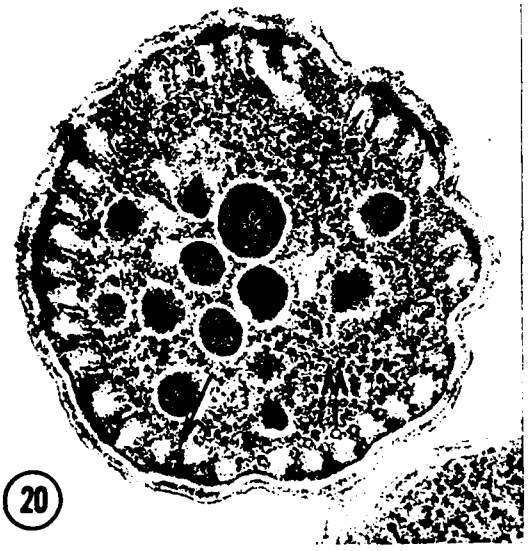

20

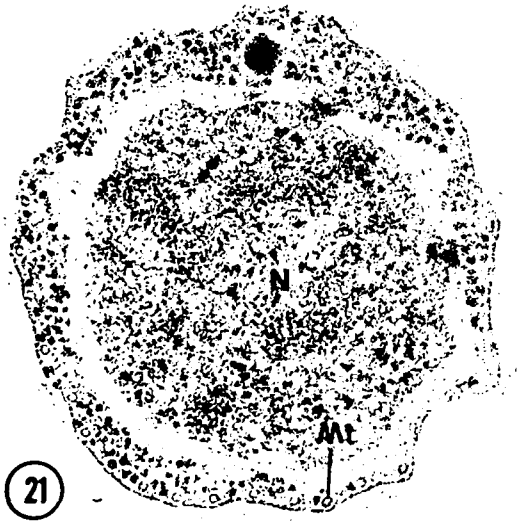

21

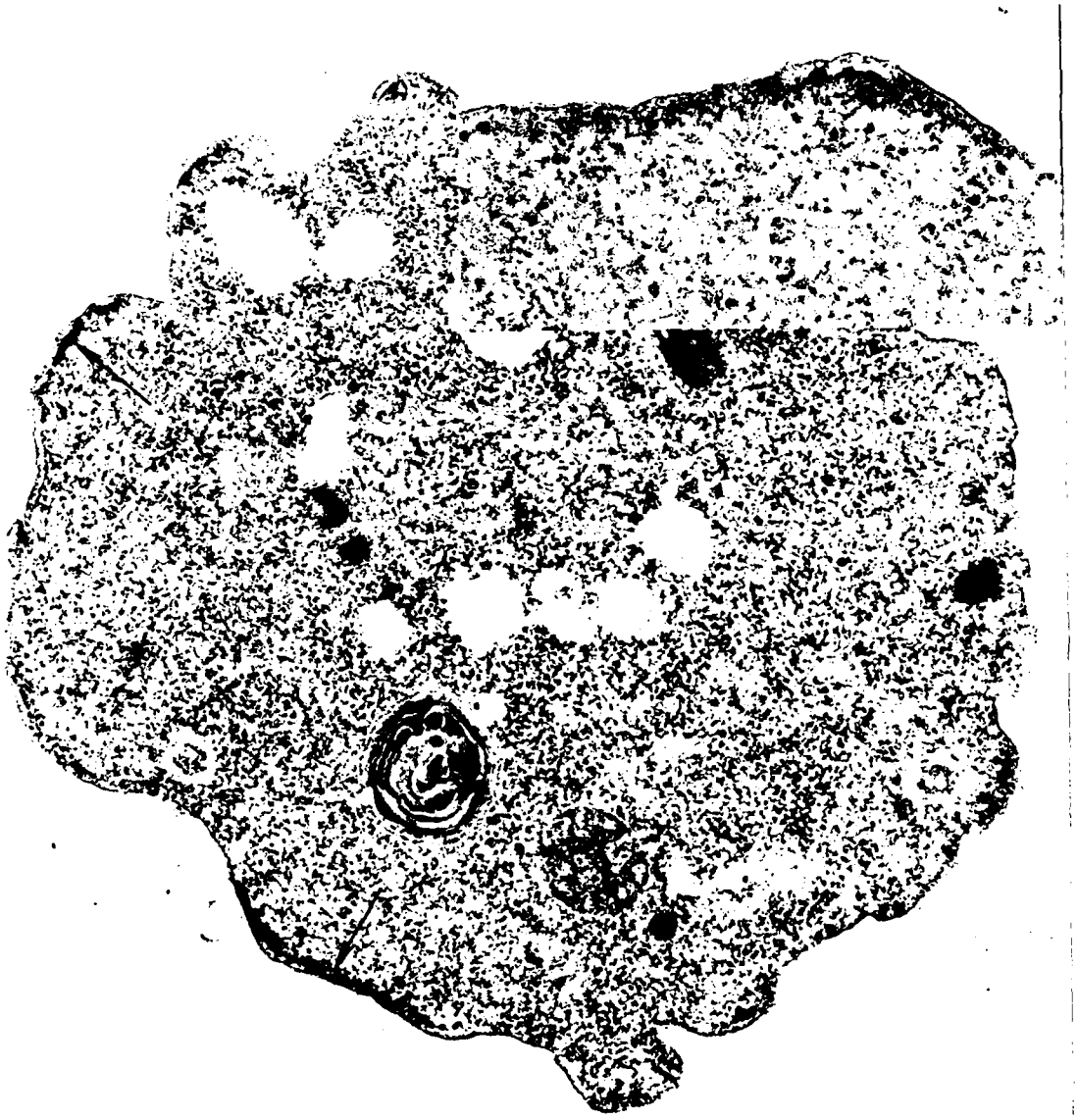

(22)

2. Update Bibliography of Published Works

a. Greenblatt, H.C., Diggs, C.L. and Aikawa, M., Antibody-dependent phagocytosis of Trypanosoma rhodesiense by murine macrophages. Am. J. Trop. Med. Hyg. 32:34-45, 1983.

b. Aikawa, M., Carter, R., Ito, M. and Nijhout, M.M., New observations on gametogenesis, fertilization, and zygote transformation in Plasmodium gallinaceum. J. Protozool. (In Press), 1983.

c. Aikawa, M., Rabbege, J.R., Udeinya, I. and Miller, L.H., Electron microscopy of knobs in P. falciparum infected erythrocytes. J. Parasitol. 62:435-437, 1983.

d. Oka, M., Aikawa, M., Freeman, R.R. and Holder, A.A., Ultrastructural localization of protective antigens of Plasmodium yoelii by the use of monoclonal antibodies and ultrathin cryomicrotomy. (Submitted for publication), 1983.

e. Berman, J.D., Oka, M. and Aikawa, M., Fine structural alterations in Trypanosoma rhodesiense treated with the prophylactic drug WR 163577 in vitro. (Submitted for publication), 1983.

f. Aikawa, M., Fine structure of malarial parasites in the various stages of development. In: Textbook of Malaria. (ed. by Wernsdorfer, W.H. and McGregor, I.A.) Churchill Livingstone, London, (In Press), 1983.

12 Copies	Director (Attn: SGRD-UWZ-AG) Walter Reed Army Institute of Research Walter Reed Army Medical Center Washington, D.C. 20012
4 Copies	HGDA (SGRD-SI) Fort Detrick Frederick, MD 21701
12 Copies	Defense Documentaion Center Attn: DDC-DCA Cameron Station Alexandria, Virginia 22314
1 Copy	Dean School of Medicine Uniformed Services University of Health Sciences 4301 Jones Bridge Road Bethesda, Maryland 20014
1 Copy	Superintendent Academy of Health Sciences U.S. Army Attn: AHS-COM Fort Sam Houston, Texas 78234

END

10-86

DTIC